

Spintronic Interface design

(スピントロニクス・インターフェース・デザイン)

Yoshio Miura

National Institute for Materials Science (NIMS)

Research Center for Magnetic and Spintronic Materials (CMSM)

Spin Theory Group

Topics

0. Introduction on spintronics

1. Spin-dependent transport in magnetic tunnel junctions with half-metallic Heusler alloys

Y. Miura, *et al.*, PRB **83**, 214411 (2011).

2. Magneto-crystalline anisotropy at interfaces of Fe(001) with MgO and MgAl₂O₄

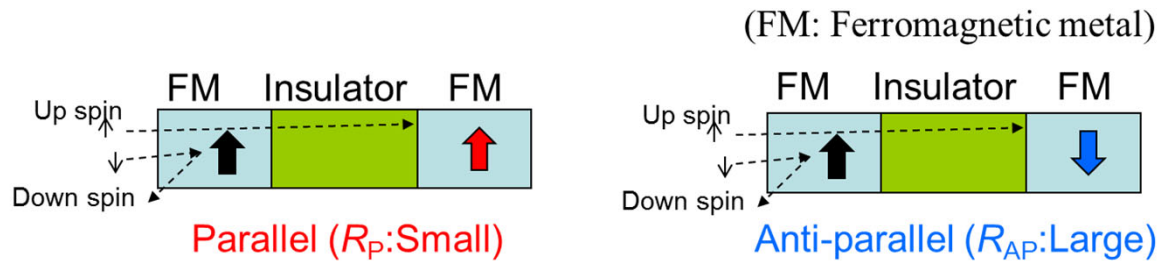
K. Masuda and Y. Miura, PRB **98**, 224421 (2018).

3. First-Principles Study on magnetic damping of Fe/MgO(001)

Y. Miura, in preparation

Introduction

Magnetic tunnel junction (MTJs)

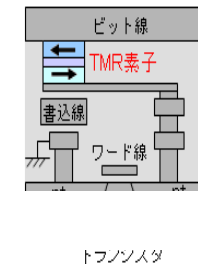
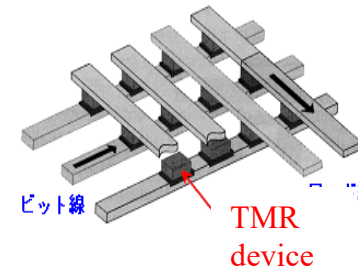


Tunneling magnetoresistance (TMR)

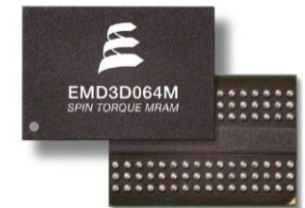
$$\text{TMR ratio} = \frac{R_{AP} - R_P}{R_{AP}}$$

Magnetoresistive Random Access Memory (MRAM)

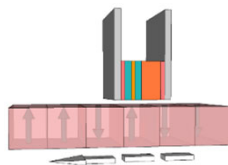
- Non volatile memory
- Fast writing speed (10~50ns)
- Low electricity consumption (~30μW)
- Long endurance (10 years)



Everspin
64Mbit MRAM



Magnetic sensor



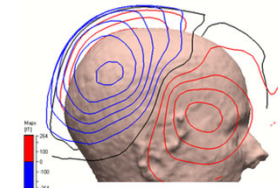
HDD read-out-head



Earth's magnetic field sensor



current sensor for car



biomagnetic sensor

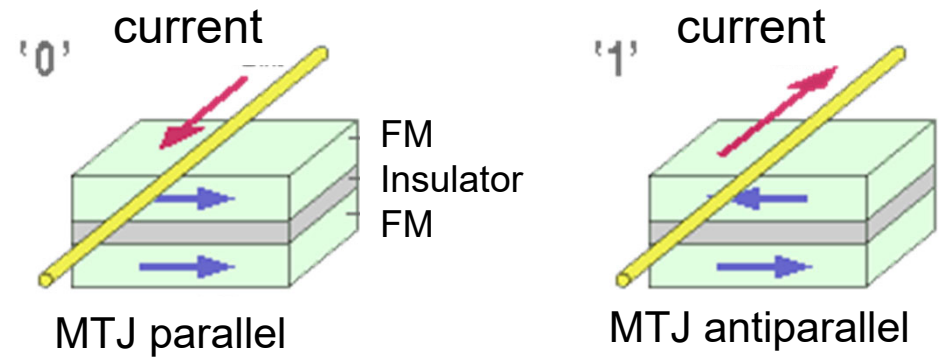
Corresponding to SQUID

Magnetization reversal in MTJs

1. Magnetic field by current

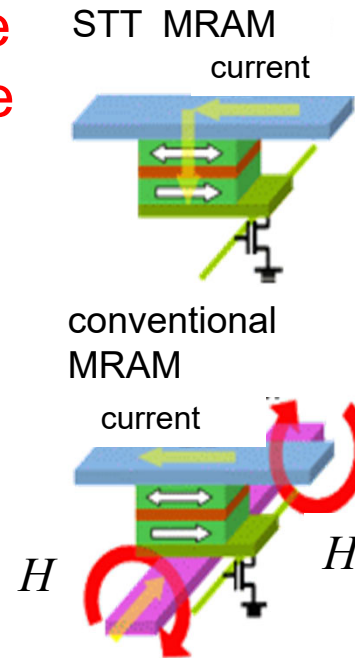
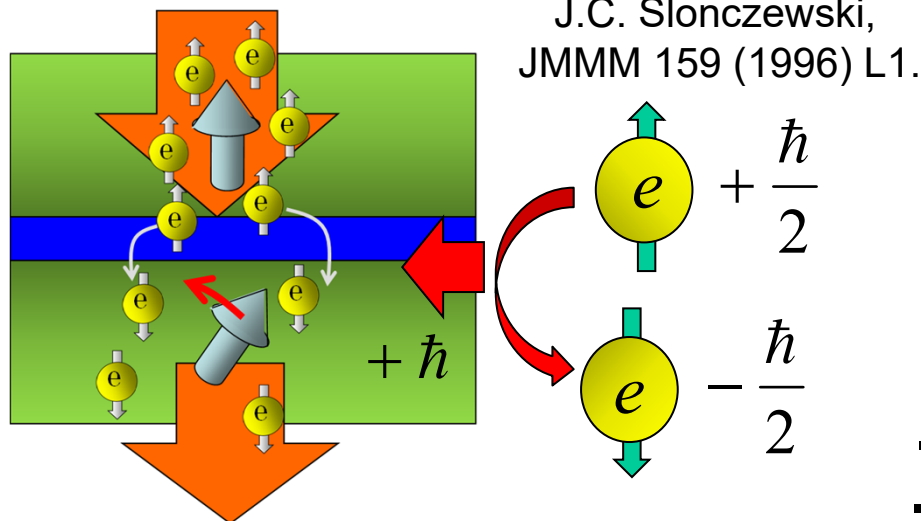
- problem:
- complicate circuit.
 - $\text{current} \propto 1/\text{device-size}$

Effects of demagnetizing field increase the critical current for writing with decreasing size of device

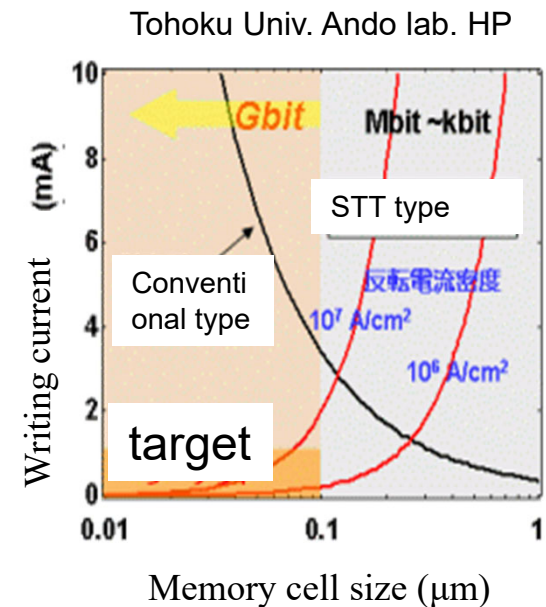


2. Spin transfer torque (STT)

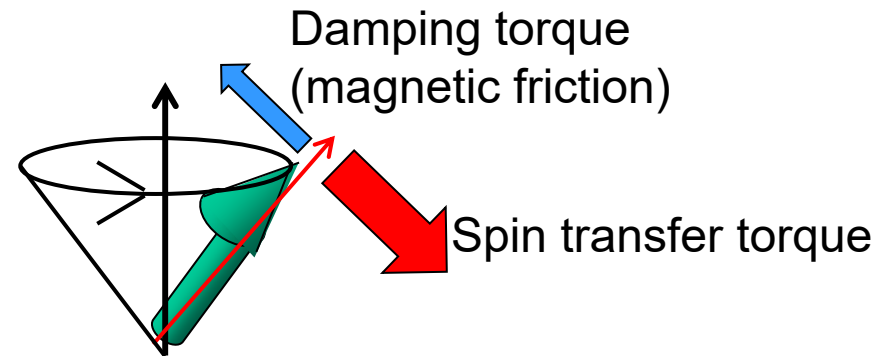
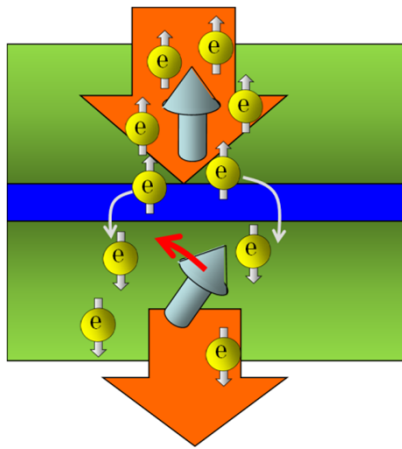
The spin flip of conductive electron give the torque to the local spin moment due to the angular momentum conservation



- simple circuit
- $\text{current} \propto \text{device-size}$



Magnetization reversal by spin transfer torque (STT)



Reduction of critical current density (J_{c0})
 ($10^7 \text{ A/cm}^2 \Rightarrow 10^5 \text{ A/cm}^2$)

$$J_{c0} \propto \alpha M_S [H_{\text{anti}} \pm 4\pi M_S] t / P$$

J.C. Slonczewski, JMMM 159 (1996) L1.

α : Magnetic damping constant
 M_S : Saturation Magnetization
 $H_{\text{anti}} \pm 4\pi M_S$: Effective anisotropy field
 P : Spin polarization
 t : Thickness of FM layer

1. High spin polarization (P)

2. Perpendicular magnetic anisotropy (PMA) $H_{\text{anti}} - 4\pi M_S$

3. Low damping constant (α)

Topics

0. Introduction on spintronics

1. Spin-dependent transport in magnetic tunnel junctions with half-metallic Heusler alloys

Y. Miura, *et al.*, PRB **83**, 214411 (2011).

2. Magneto-crystalline anisotropy at interfaces of Fe(001) with MgO and MgAl₂O₄

K. Masuda and Y. Miura, PRB **98**, 224421 (2018).

3. First-Principles Study on magnetic damping of Fe/MgO(001)

Y. Miura, in preparation

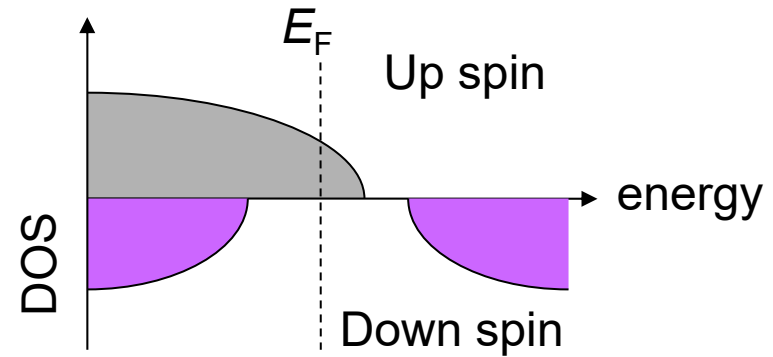
Introduction: Half-metallic ferromagnetic

Julliere model

$$\text{TMR} = \frac{G_P - G_{AP}}{G_P} = \frac{2P_L \cdot P_R}{1 - P_L \cdot P_R}$$

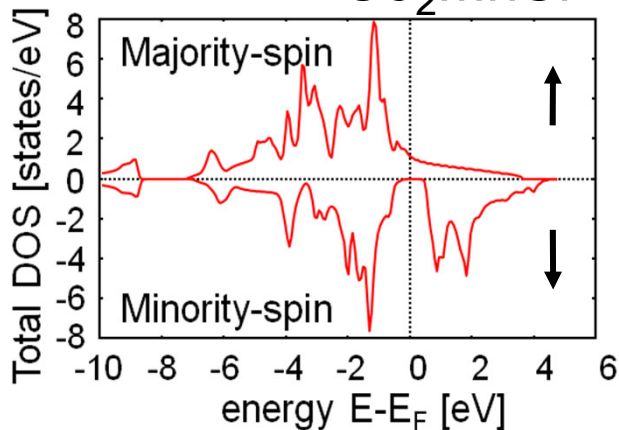
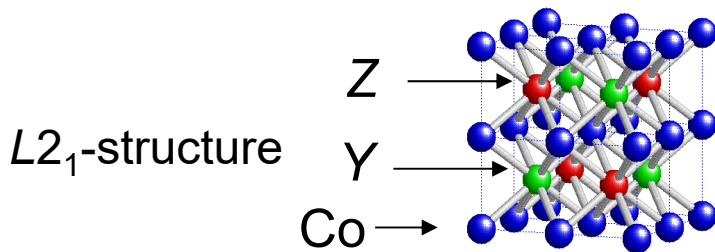
Spin-polarization at E_F $P_{L(R)} = \frac{D_{L(R)}^\uparrow - D_{L(R)}^\downarrow}{D_{L(R)}^\uparrow + D_{L(R)}^\downarrow}$

The Half-metallic ferromagnets

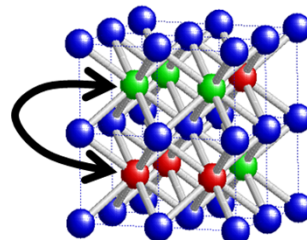


Co-based full Heusler alloys

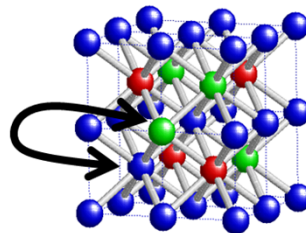
Co_2YZ ($Y=\text{Fe}, \text{Mn}, \text{Cr}$; $Z=\text{Si}, \text{Ge}, \text{Al}, \text{Ga}$)



(1) B2-type disorder

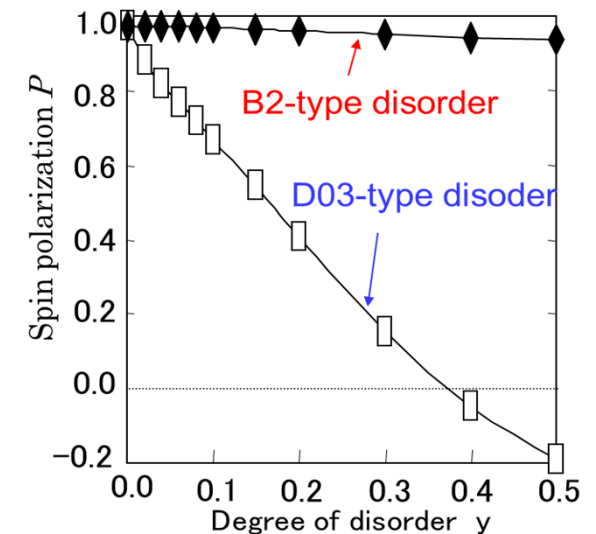


(2) D03-type disorder



High Curie temperature (900K)

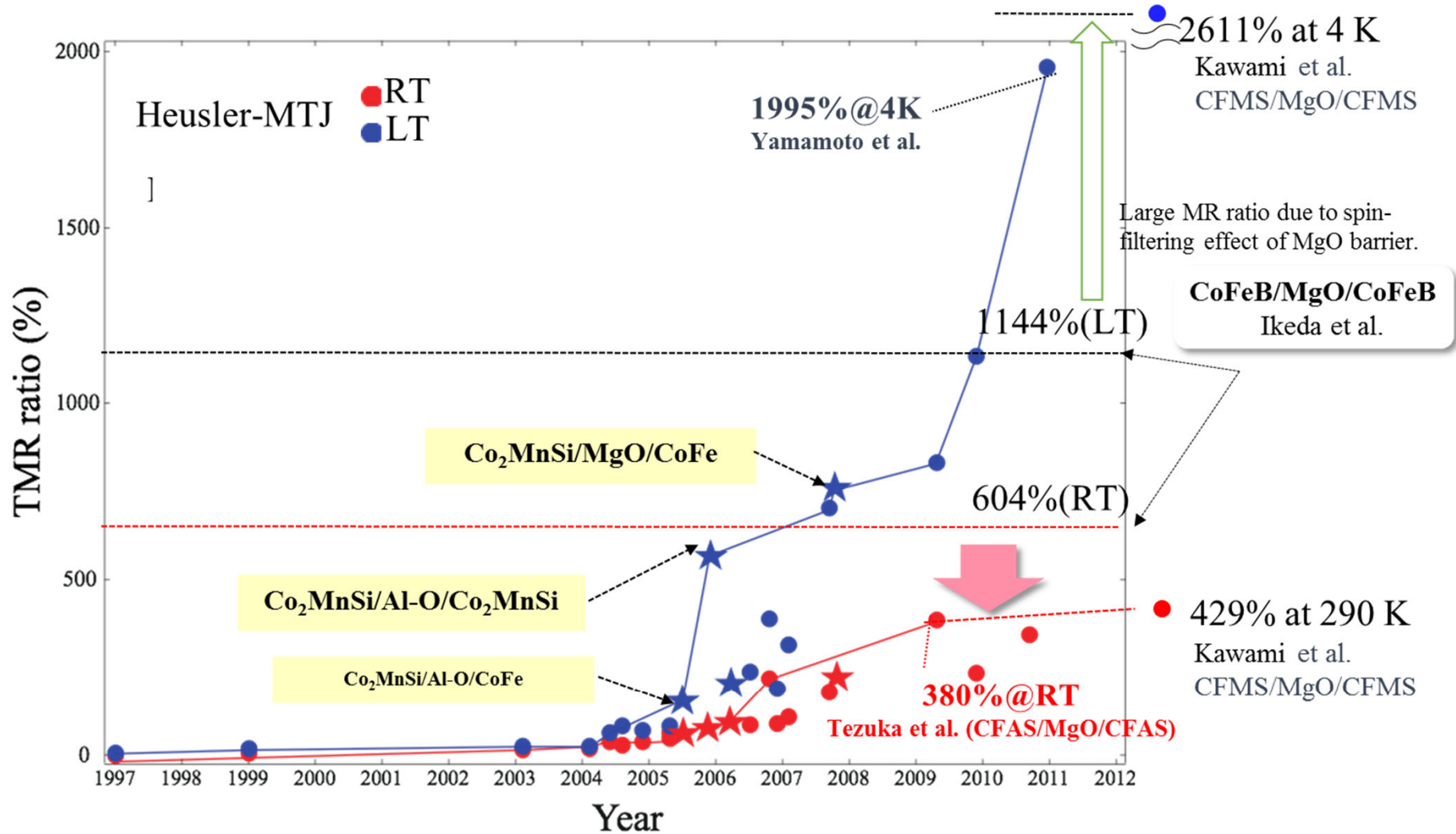
Simple fabrication process



Problem in MTJs with half-metallic Heusler alloys

Progress of TMR ratio in Heusler-based MTJ

Courtesy of Dr. Sakuraba

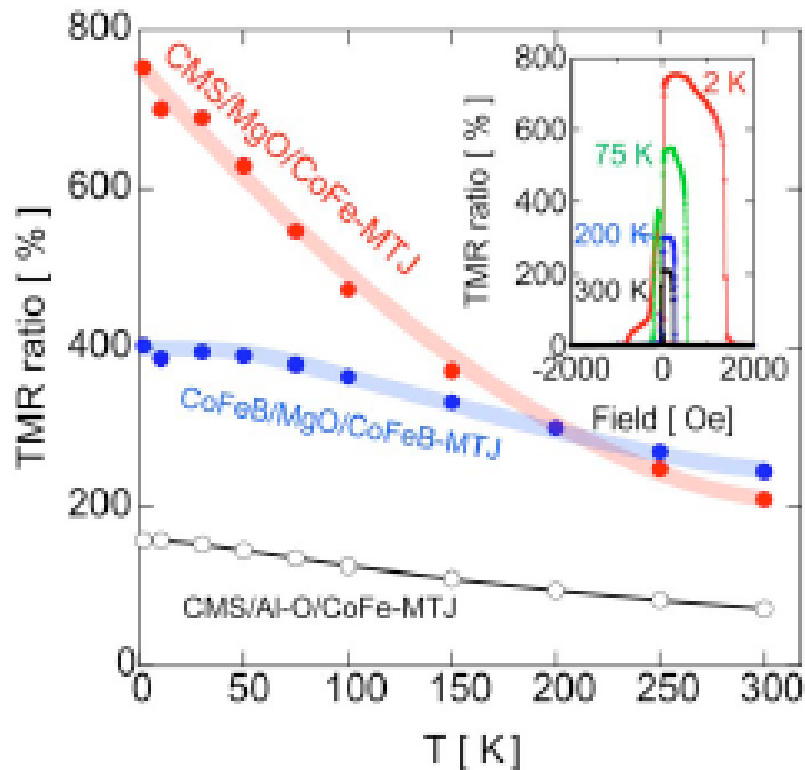


Heusler-based MTJ : Large temperature dependence of MR ratio is still a serious problem especially in CMS.

CMS: Co₂MnSi CFAS: Co₂Fe(AlSi) CFMS: Co₂(FeMn)Si

Problem in MTJs with half-metallic Heusler alloys

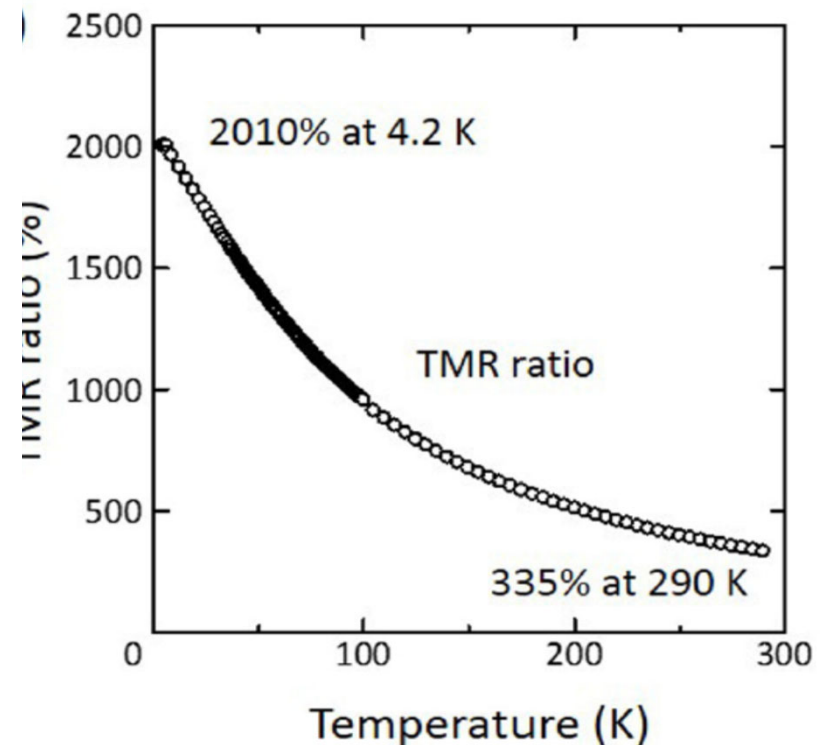
TMR ratio of MTJs with Co_2MnSi (CMS)



S. Tsunegi, *et al.*, APL 93 (2008) 112506.

CMS/MgO/CMS(001)

B. Hu, *et al.*, PRB 94 (2016) 094428.



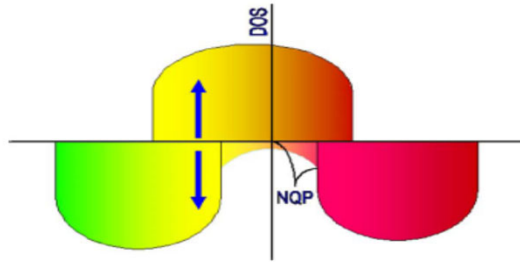
Present top data

Problem: Reduction of the TMR ratio at room temperature

in spite of high curie temperature of Co_2MnSi : 985K

Introduction (theory)

1. Temperature dependence of bulk density of states owing to non-quasiparticle

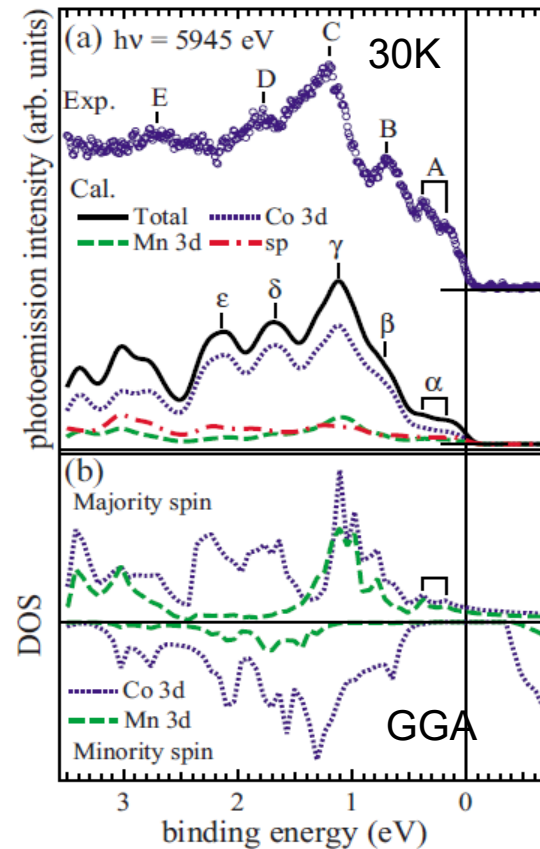
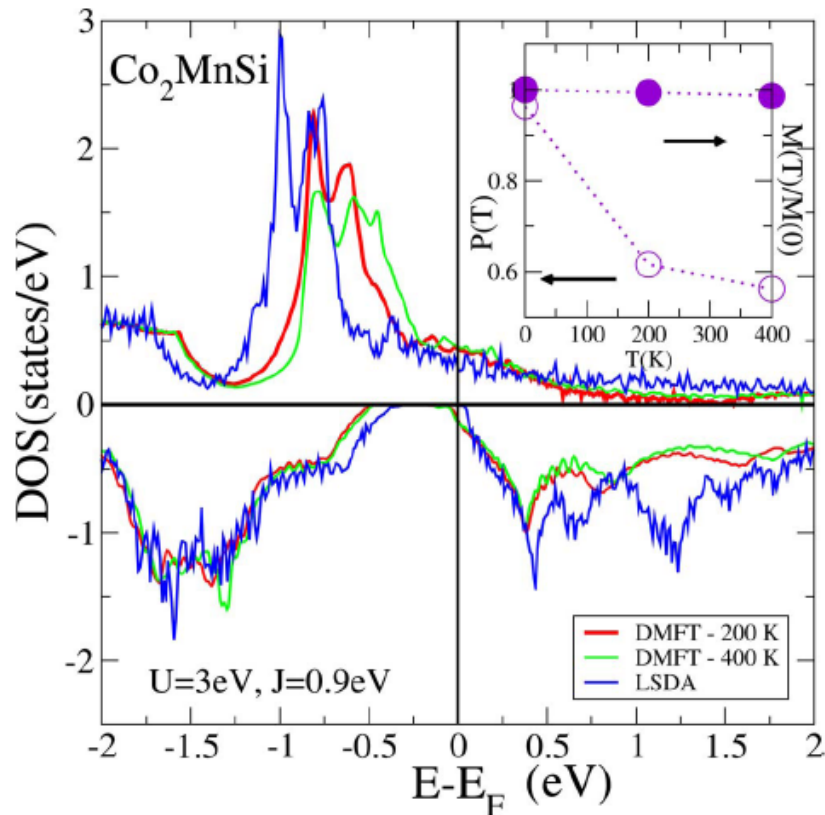


M. I. Katsnelson, *et al.*, Rev. Mod. Phys. **80**, 315 (2008).

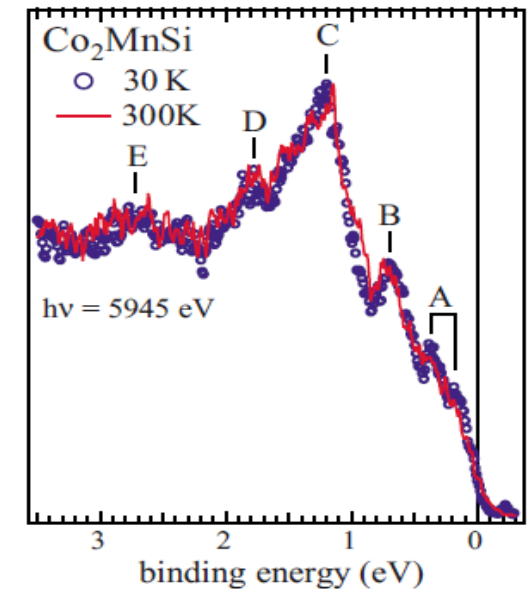
X-ray photoelectron spectroscopy of bulk CMS

K. Miyamoto, *et al.*, PRB. **79**, 100405(R) (2009).

Temperature dependence of total DOS of bulk CMS calculated from DMFT



Valence band electronic structures of bulk CMS

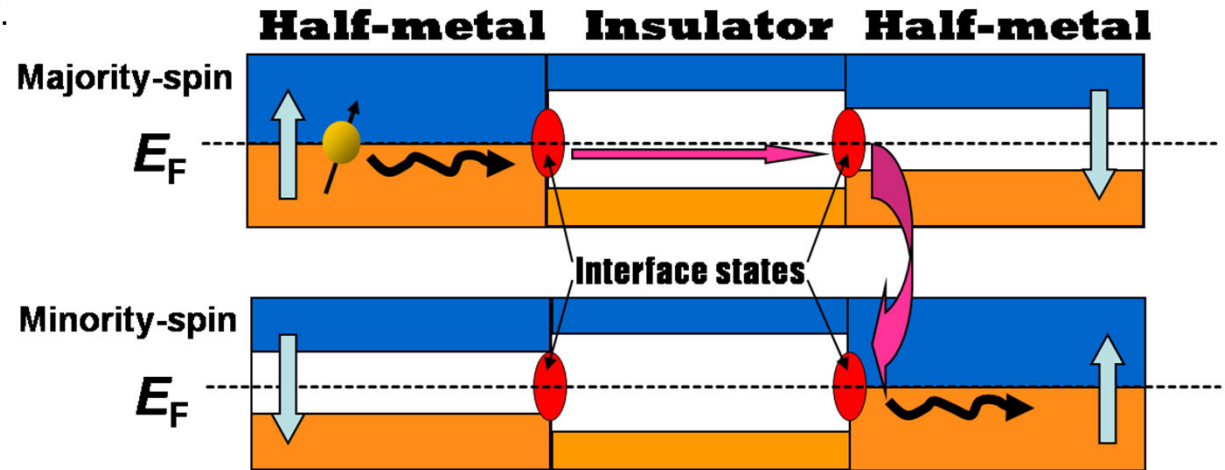


Introduction (theory)

2. **Effects of** the spin-flip scattering through the interface states promoted by magnetic excitation.

P. Mavropoulos, *et al.*, PRB, 72 (2005) 174428.

Anti-parallel magnetization

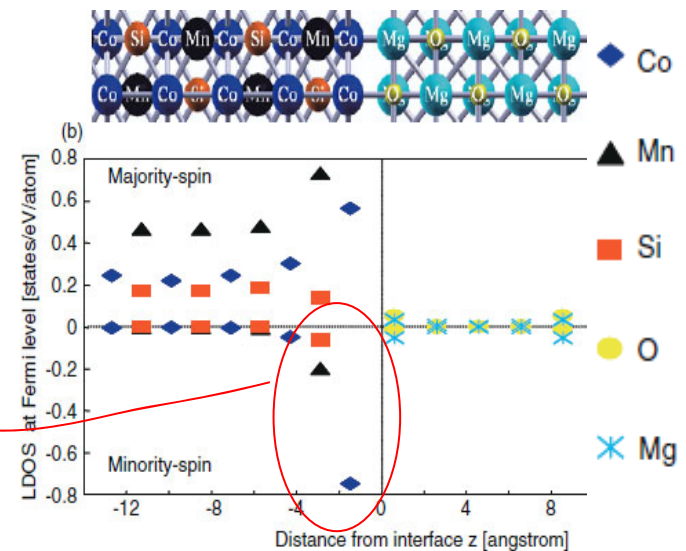
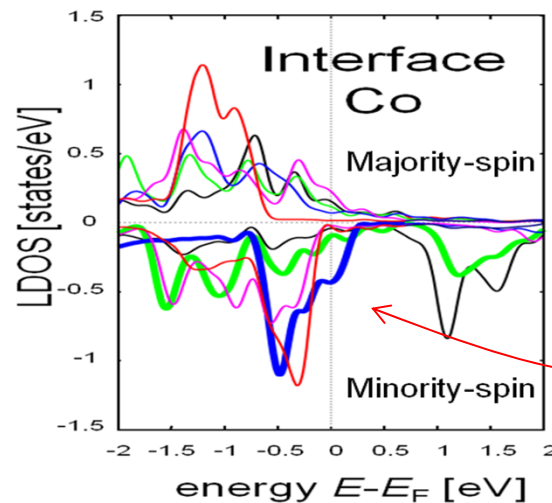


Co₂MnSi/MgO(001)

Y. Miura, *et al.*, PRB 78, 064416 (2008).

Y. Miura, *et al.*, JPCM 19, 365228 (2007).

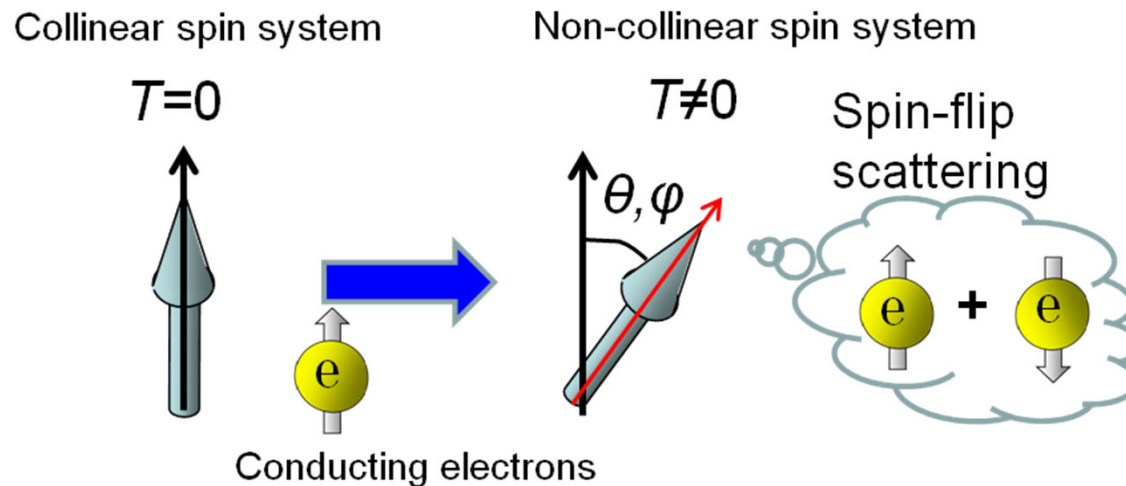
Co d_{z^2} — Δ_1
 Co $d_{x^2-y^2}$ — Δ_2
 Co d_{xy} — Δ_3
 Co d_{zx} — Δ_4
 Co d_{yz} — Δ_5



Purpose of this work

- To clarify a possible origin of reduction of TMR ratio at RT in MTJ with half-metallic Heusler alloys,
- We investigate effects of spin-flip scattering through the interface states at CMS/MgO junctions originating from non-collinear magnetic structures.

Thermal fluctuation of local spin-moments \Rightarrow Non-collinear magnetic structures



Calculation Method

Electronic structures

PWSCF <http://www.pwscf.org/>

- ◆ Plane-wave basis set
- ◆ Ultra-soft pseudopotential method
- ◆ GGA for Exchange-Correlation term

Transport calculations

$$G = \frac{e^2}{h} \sum_i^N T_i$$

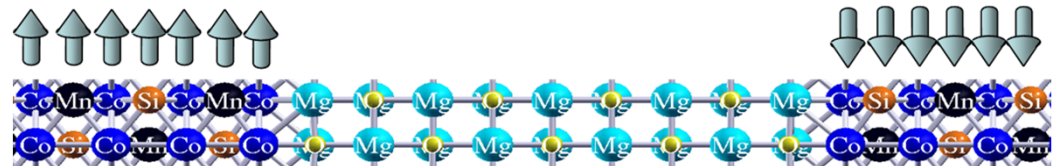
- ◆ Landauer formula
- ◆ Zero bias limit Ballistic Conductance

H. J. Choi and J. Ihm, PRB 59 (1999) 2267.

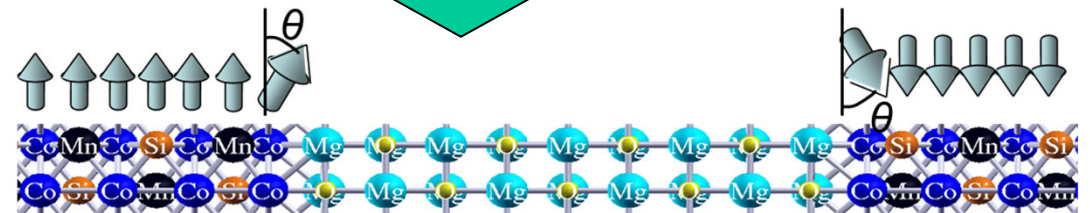
A. Smogunov, A. Dal Corso and E. Tosatti, PRB 70 (2004) 045417.

Conductance calculation in Non-collinear spin system

First, we perform electronic structure calculations in collinear spin system



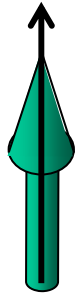
Then, we artificially rotate spin-quantum axis of local spin-moments to obtain density-matrix in non-collinear spin system.



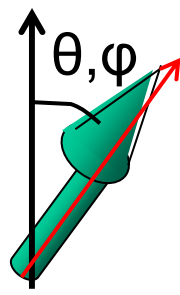
The rotation of spin-quantum axis in NC spin system

The density matrix in non-collinear spin system is obtained from the inverse unitary transformation of spin-density in collinear spin system.

Collinear spin system(\mathbf{n}_i)



Non-collinear spin system($\mathbf{n}_{\alpha\beta}$)



$$\mathbf{n}_{\alpha\beta}(\mathbf{r}) = \sum_{i=(\uparrow,\downarrow)} U_{\alpha i}^+ \mathbf{n}_i(\mathbf{r}) U_{i\beta}$$

$$U = \begin{pmatrix} \exp(\frac{1}{2}i\varphi)\cos(\frac{1}{2}\theta) & \exp(-\frac{1}{2}i\varphi)\sin(\frac{1}{2}\theta) \\ -\exp(\frac{1}{2}i\varphi)\sin(\frac{1}{2}\theta) & \exp(-\frac{1}{2}i\varphi)\cos(\frac{1}{2}\theta) \end{pmatrix}$$

J. Kubler et al., J. Phys. F: Met. Phys. **18**, 469 (1988).

Local potential in Collinear spin system

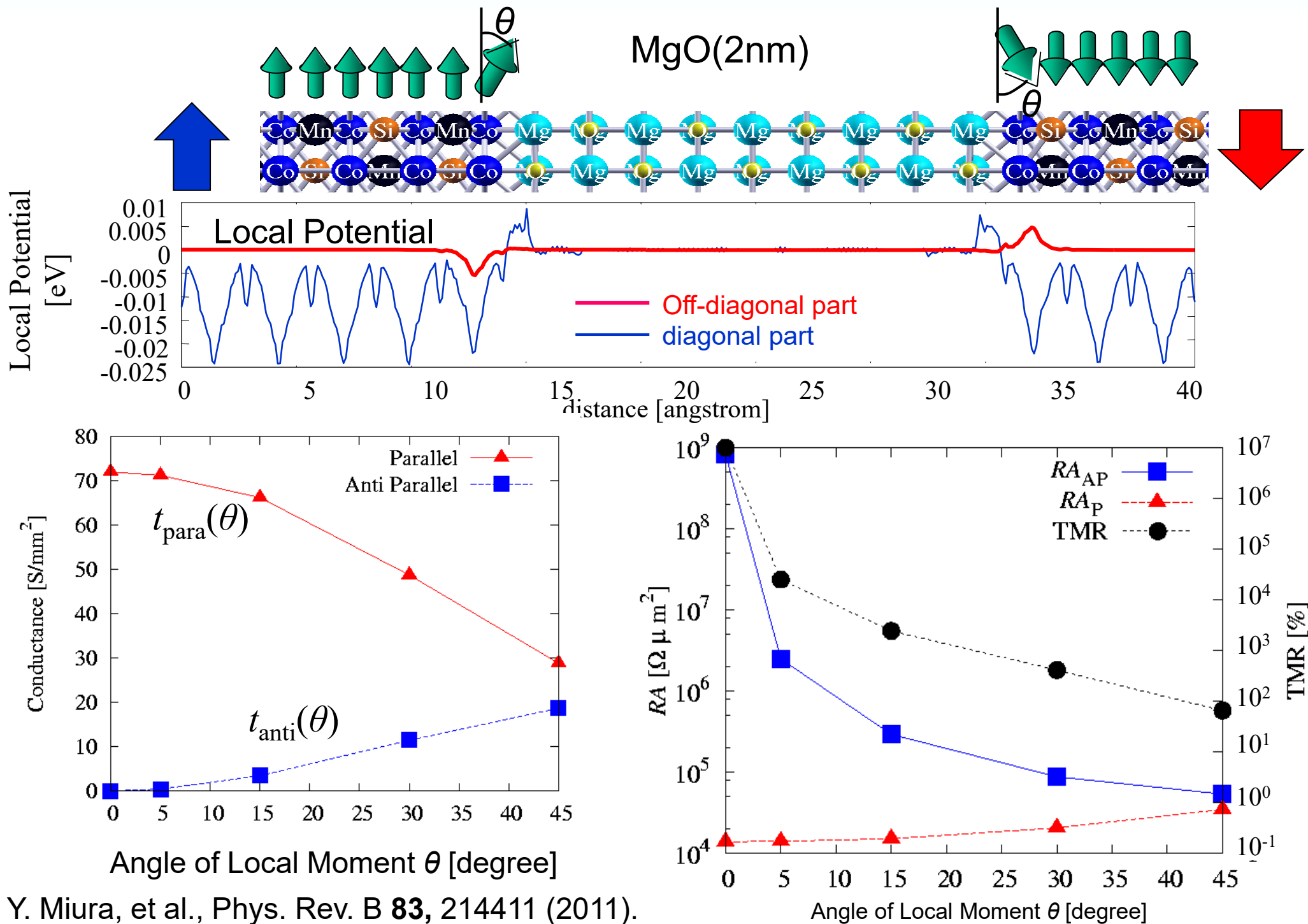
$$\begin{pmatrix} V_L(r)+V_H(r)+\frac{1}{2}\sum_{\alpha=(\uparrow,\downarrow)}\frac{\delta E_{XC}}{\delta n_{\alpha}}+\frac{1}{2}\left(\frac{\delta E_{XC}}{\delta n_{\uparrow}}-\frac{\delta E_{XC}}{\delta n_{\downarrow}}\right) & 0 \\ 0 & V_L(r)+V_H(r)+\frac{1}{2}\sum_{\alpha=(\uparrow,\downarrow)}\frac{\delta E_{XC}}{\delta n_{\alpha}}-\frac{1}{2}\left(\frac{\delta E_{XC}}{\delta n_{\uparrow}}-\frac{\delta E_{XC}}{\delta n_{\downarrow}}\right) \end{pmatrix}$$

Local potential in Non-Collinear spin system

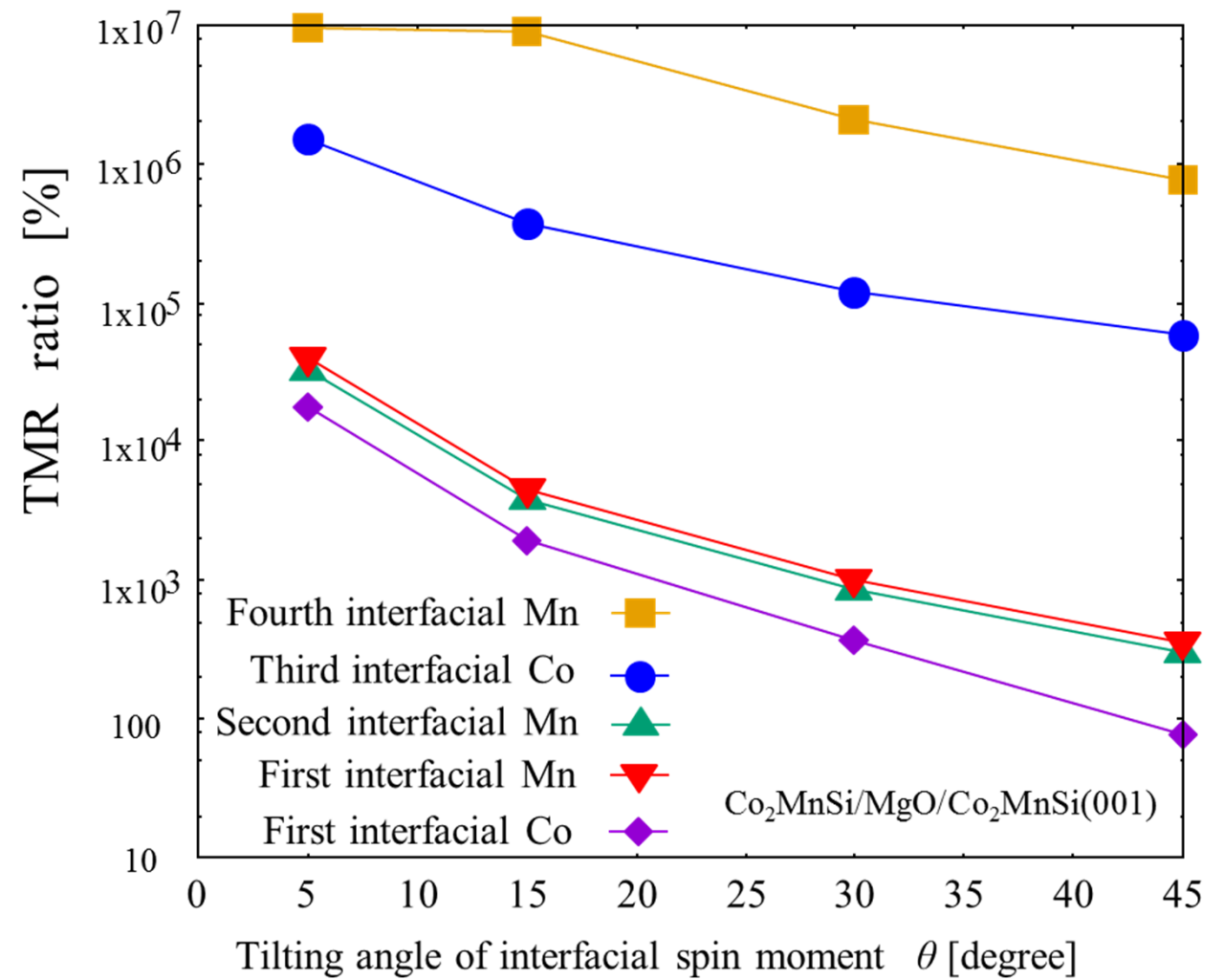
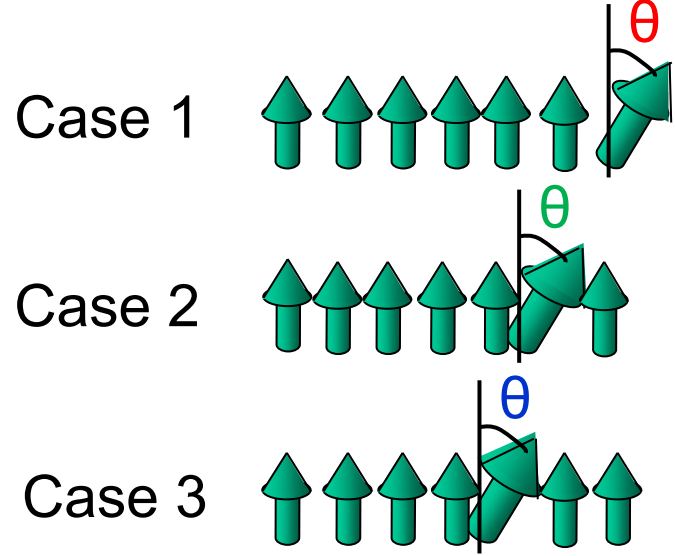
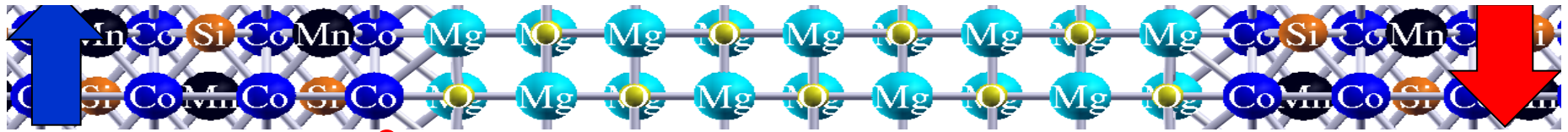
$$\begin{pmatrix} V_L(r)+V_H(r)+\frac{1}{2}\sum_{\alpha=(\uparrow,\downarrow)}\frac{\delta E_{XC}}{\delta n_{\alpha}}+\frac{1}{2}\left(\frac{\delta E_{XC}}{\delta n_{\uparrow}}-\frac{\delta E_{XC}}{\delta n_{\downarrow}}\right)\cos\theta & \frac{1}{2}\left(\frac{\delta E_{XC}}{\delta n_{\uparrow}}-\frac{\delta E_{XC}}{\delta n_{\downarrow}}\right)\sin\theta\cos\phi+\frac{i}{2}\left(\frac{\delta E_{XC}}{\delta n_{\uparrow}}-\frac{\delta E_{XC}}{\delta n_{\downarrow}}\right)\sin\theta\sin\phi \\ \frac{1}{2}\left(\frac{\delta E_{XC}}{\delta n_{\uparrow}}-\frac{\delta E_{XC}}{\delta n_{\downarrow}}\right)\sin\theta\cos\phi-\frac{i}{2}\left(\frac{\delta E_{XC}}{\delta n_{\uparrow}}-\frac{\delta E_{XC}}{\delta n_{\downarrow}}\right)\sin\theta\sin\phi & V_L(r)+V_H(r)+\frac{1}{2}\sum_{\alpha=(\uparrow,\downarrow)}\frac{\delta E_{XC}}{\delta n_{\alpha}}-\frac{1}{2}\left(\frac{\delta E_{XC}}{\delta n_{\uparrow}}-\frac{\delta E_{XC}}{\delta n_{\downarrow}}\right)\cos\theta \end{pmatrix}$$

Y. Miura, et al., Phys. Rev. B **83**, 214411 (2011).

Transport in non-collinear spin MTJs



Effects of sub-interfacial non-collinear spin to TMR

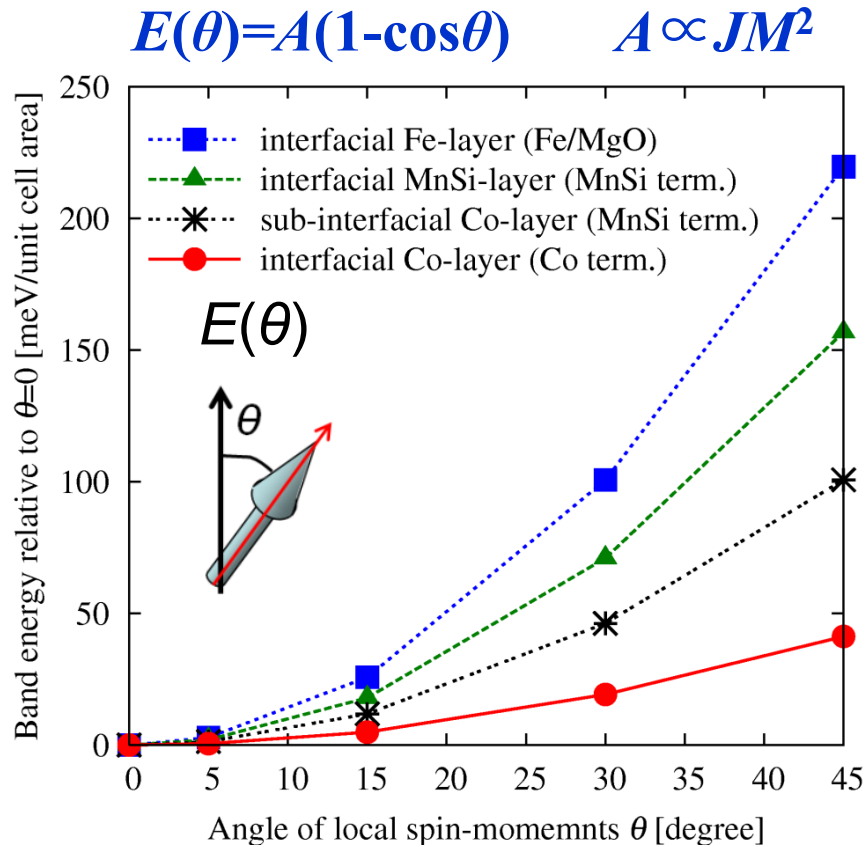


Noncollinear magnetic structures of the first and the second interfacial layer strongly reduce TMR.

Noncollinear magnetic structure of the third and fourth interfacial layer show relatively small reduction of TMR.

Exchange stiffness constant at CMS/MgO(001)

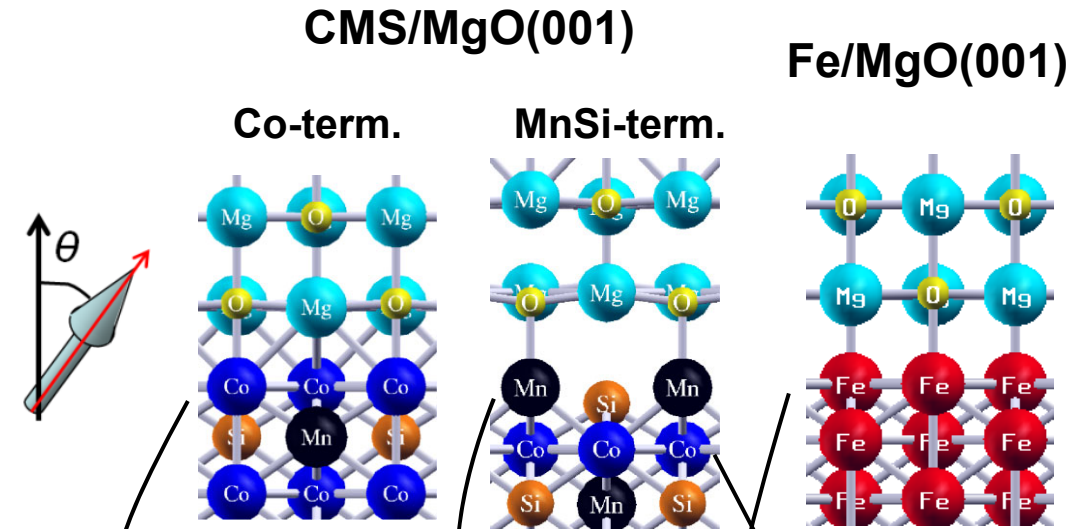
Increase of band energy of Non-collinear Spin \Rightarrow Strength of exchange coupling



A. Sakuma, *et al.*, JAP **105**, 07C910 (2009).

Off-diagonal part of local potential

$$V_{\alpha\beta(\alpha\neq\beta)}(\mathbf{r}) = \left(\frac{\delta E_{XC}}{\delta n_{\uparrow}} - \frac{\delta E_{XC}}{\delta n_{\downarrow}} \right) \sin \theta$$



Exchange stiffness of interfacial atoms

A [meV/u.c.a.]	Co ¹	Mn ¹	Fe ¹	Co ²
Bulk (CMS or Fe)	414	529	600	414
MgO interface	<u>145</u>	<u>565</u>	<u>753</u>	<u>347</u>
ΔA [meV/u.c.a.]	-269	+34	+153	-67

Interfacial local spin-moment

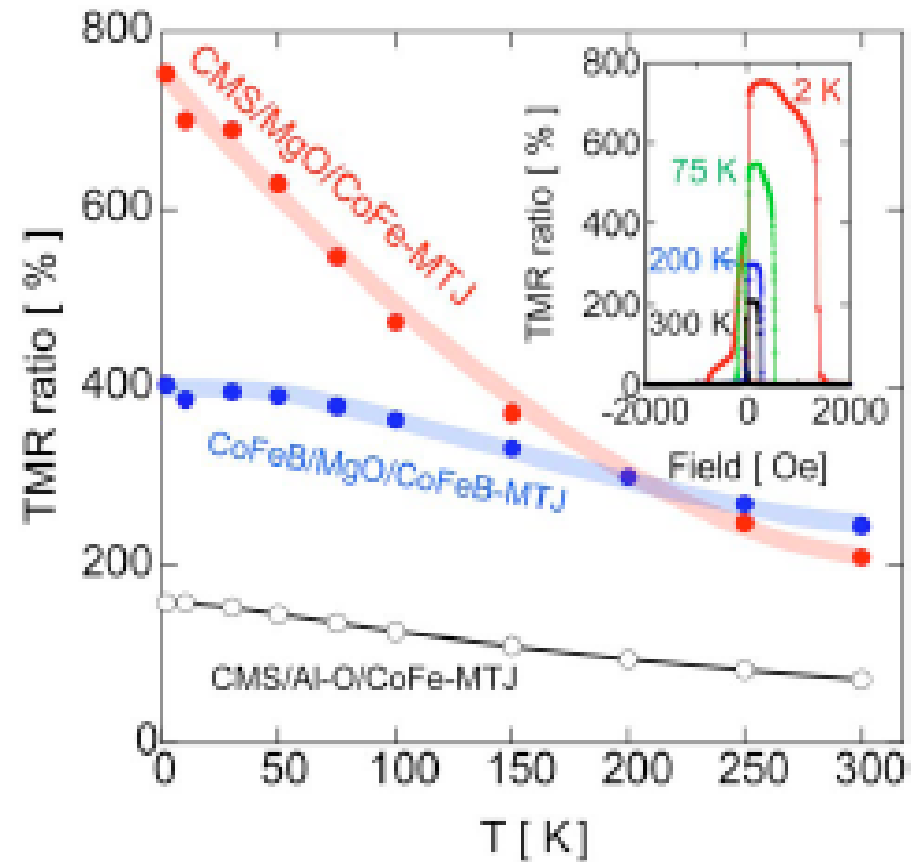
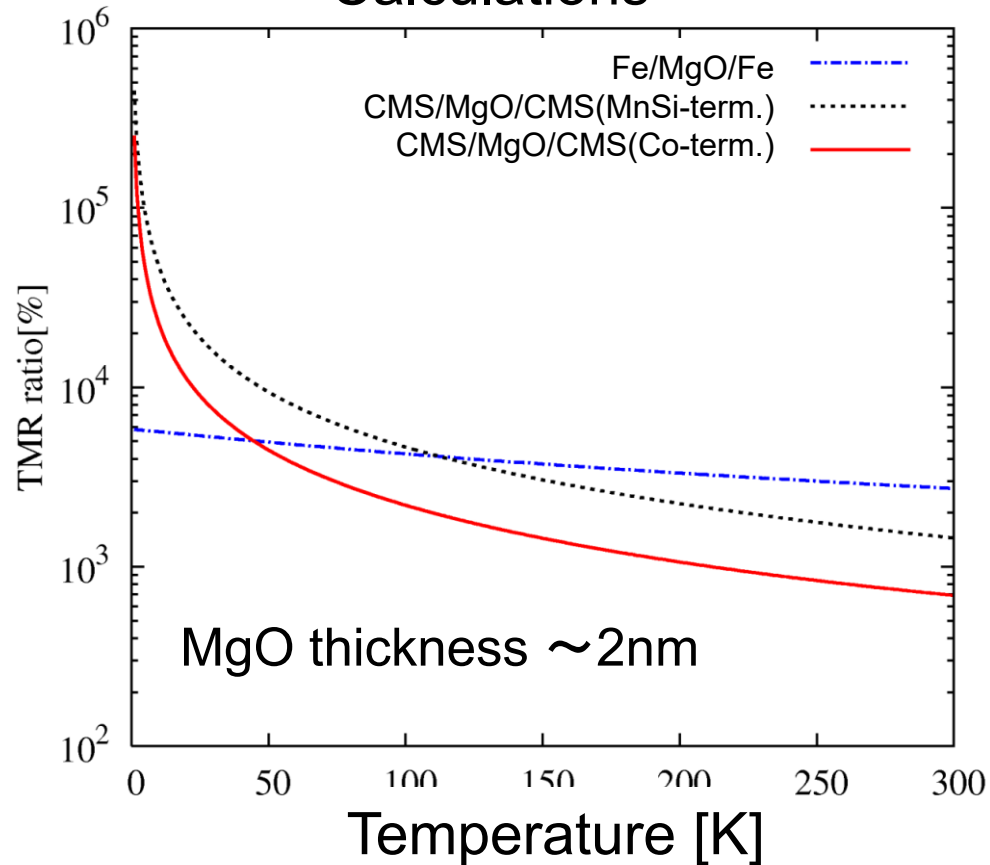
M [μ_B]	Co ¹	Mn ¹	Fe ¹
Bulk (CMS or Fe)	0.93	3.31	2.35
MgO interface	<u>0.54</u>	<u>4.06</u>	<u>2.98</u>
ΔM [μ_B]	-0.39	+0.75	+0.63

TMR ratio at finite temperature

Boltzmann average of tunneling conductance

$$t^{(\text{para,anti})}(T) = \frac{\int t_{(\text{para,anti})}(\theta) \exp[-2E(\theta)/k_B T] \sin \theta d\theta}{\int \exp[-2E(\theta)/k_B T] \sin \theta d\theta}$$

Calculations

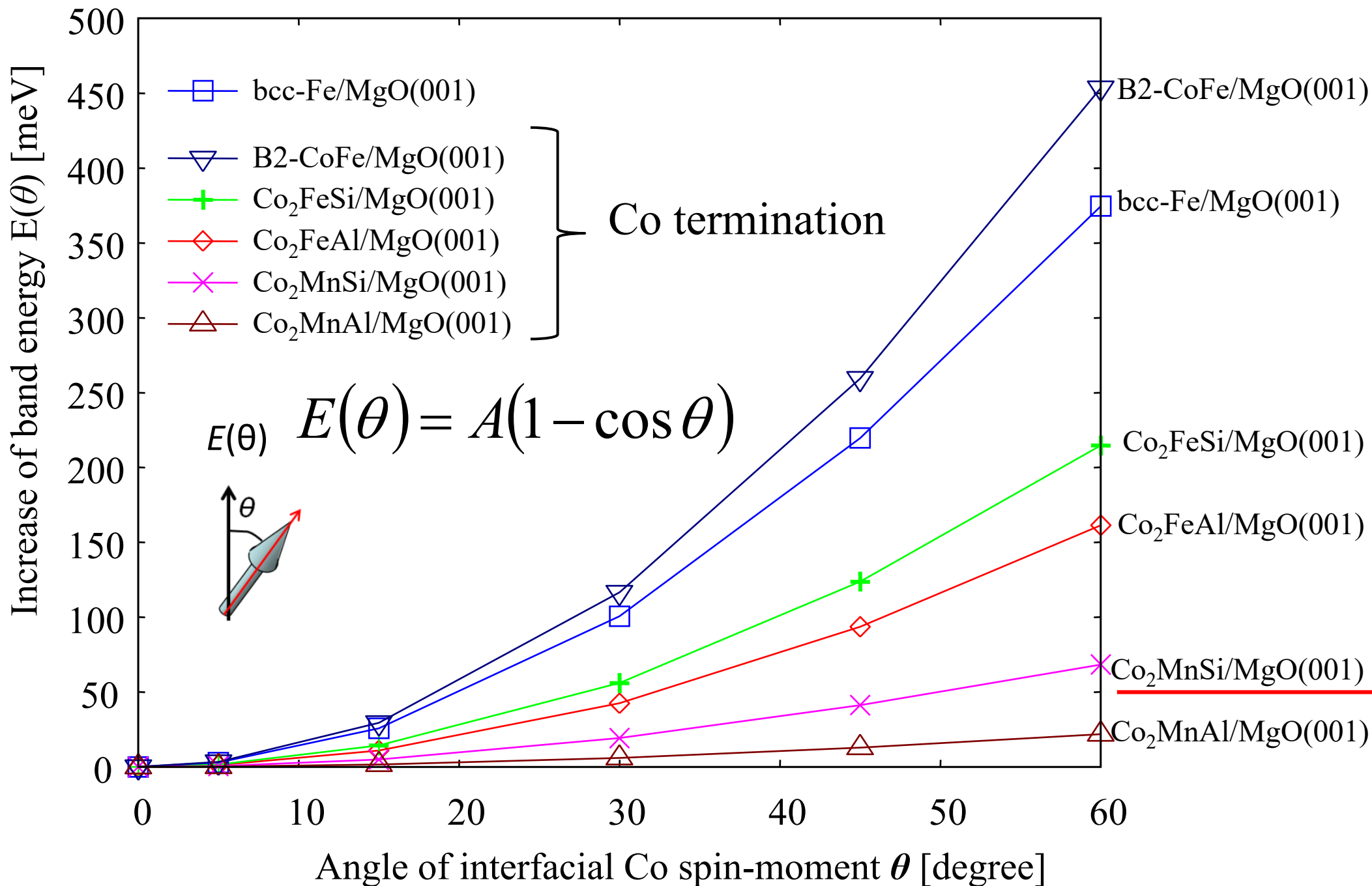


S. Tsunegi, *et al.*, APL 93 (2008) 112506.

Reduction TMR ratio at RT in CMS/MgO/CMS MTJ can be attributed to a spin-flip scattering at interfacial region caused by thermal fluctuation.

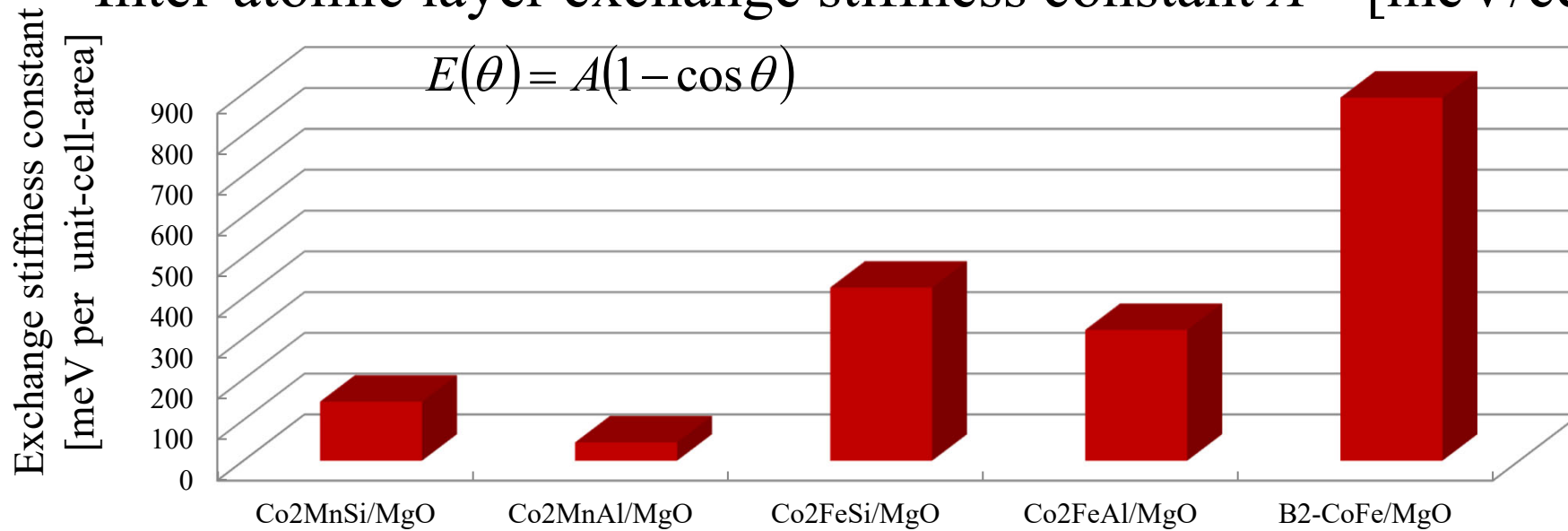
Exchange coupling for other Heusler alloys

Pwscf with GGA

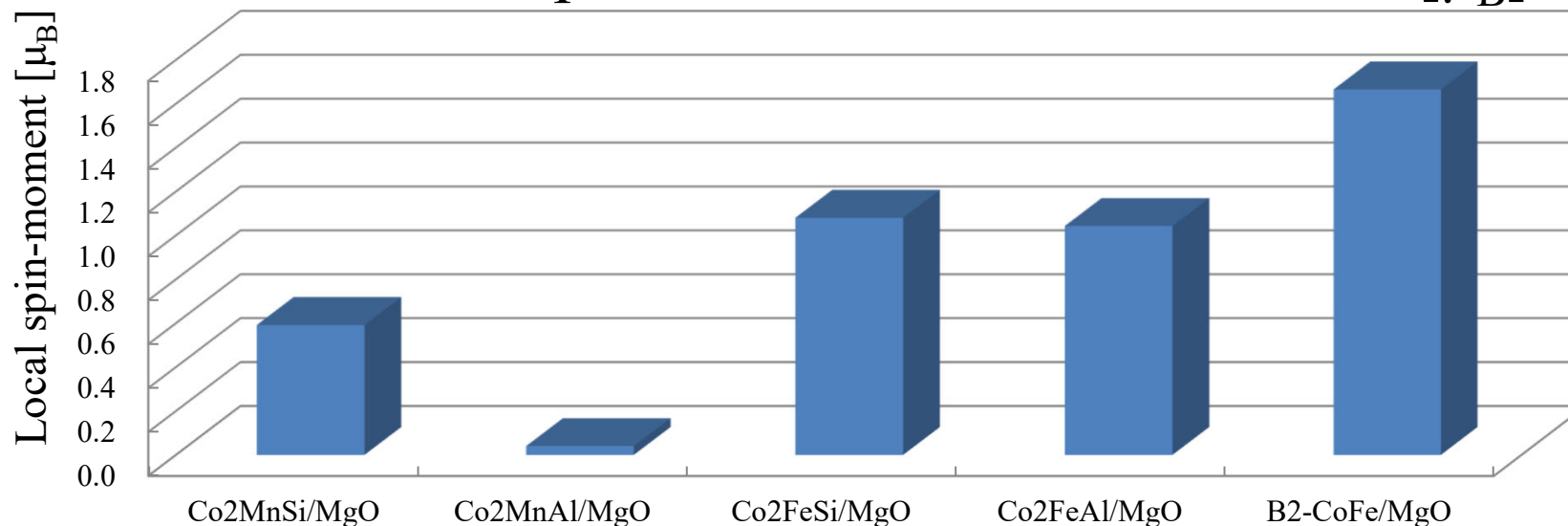


Exchange stiffness constant at Co termination

Inter-atomic layer exchange stiffness constant A [meV/cell area]



Interfacial Co spin-moment at Co termination [μ_B] $A \propto JM^2$



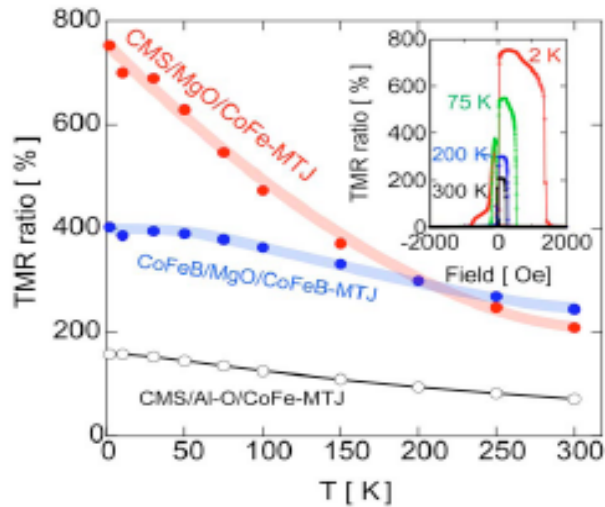
Enhancement of interfacial Co spin-moment is effective to obtain large exchange coupling.

Comparison with Experimental results on TMR at LT and RT

Co₂MnSi/MgO(001)

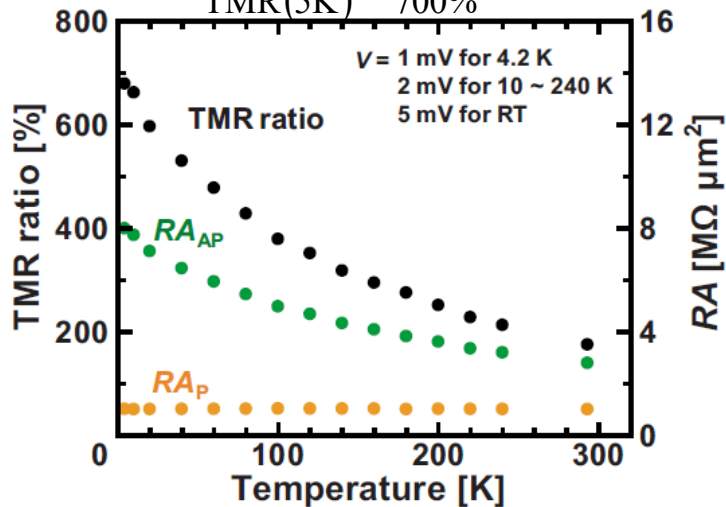
S. Tsunegi, *et al.*, APL 93 (2008) 112506.

$$\frac{\text{TMR}(\text{RT})}{\text{TMR}(2\text{K})} = \frac{217\%}{753\%} = 0.29$$



T. Ishikawa, *et al.*, APL 94 (2009) 092503.

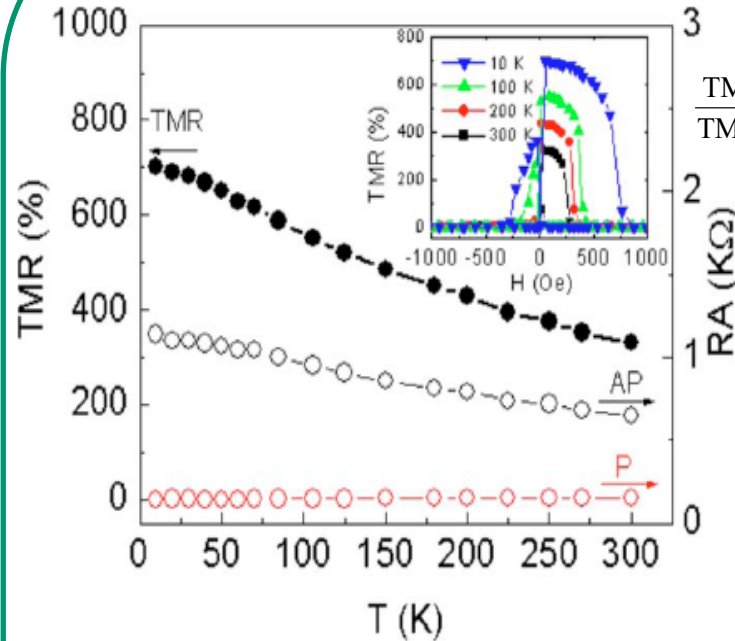
$$\frac{\text{TMR}(\text{RT})}{\text{TMR}(5\text{K})} = \frac{180\%}{700\%} = 0.26$$



Co₂Fe(Al,Si)/MgO(001)

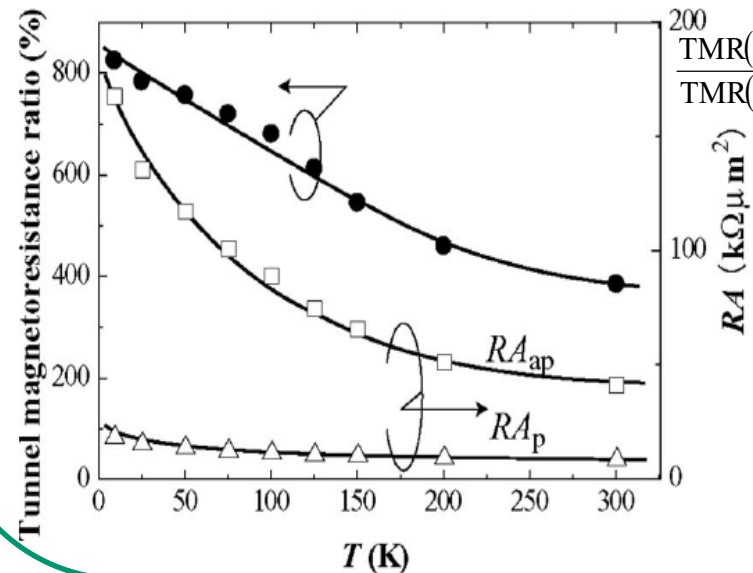
W. Wang, *et al.*, APL 95 (2009) 182502.

$$\frac{\text{TMR}(\text{RT})}{\text{TMR}(10\text{K})} = \frac{330\%}{700\%} = 0.47$$

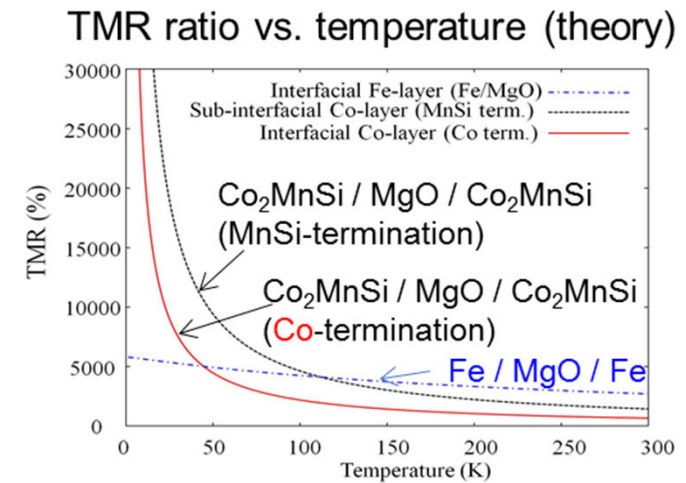
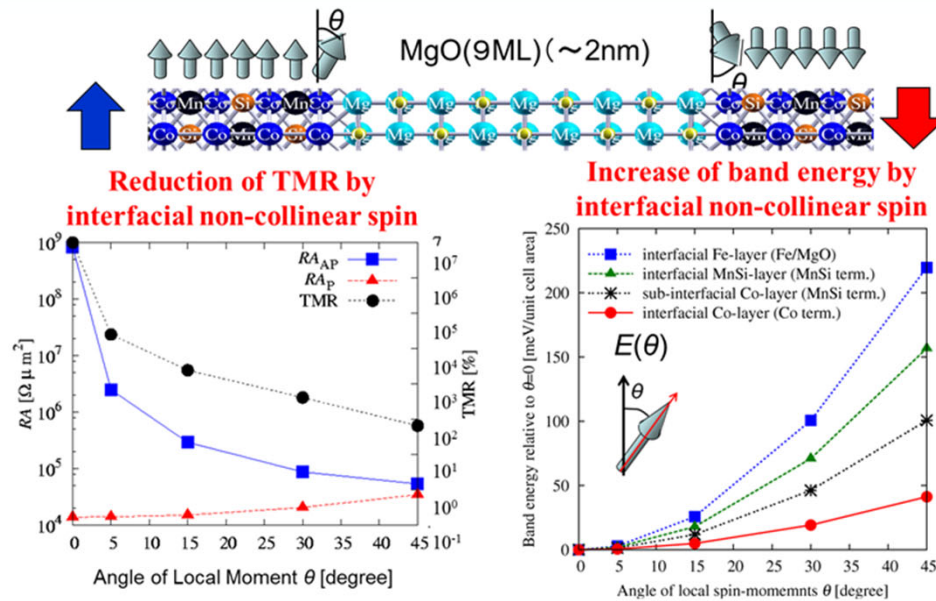


N. Tezuka, *et al.*, APL 94 (2009) 162504.

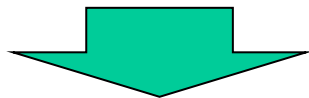
$$\frac{\text{TMR}(\text{RT})}{\text{TMR}(9\text{K})} = \frac{386\%}{832\%} = 0.46$$



Summary of the first topic



- ◇ Spin-flip scattering at 1ML of interfacial non-collinear magnetic structures strongly affect the spin-dependent conductance and TMR ratio.
- ◇ Interfacial Co-layer is easy to fluctuate at RT due to the small exchange stiffness at CMS/MgO(001) junctions.
- ◇ The reduction of the TMR ratio at RT can be attributed to spin-flip scattering at interfacial region caused by thermal fluctuation of interfacial Co-layers.



To raise the TMR ratio at RT, we have to insert CoFe-layer to enhance the interfacial exchange stiffness of CMS/MgO junction.

Topics

0. Introduction on spintronics

1. Spin-dependent transport in magnetic tunnel junctions with half-metallic Heusler alloys

Y. Miura, *et al.*, PRB **83**, 214411 (2011).

2. Magneto-crystalline anisotropy at interfaces of Fe(001) with MgO and MgAl₂O₄

K. Masuda and Y. Miura, PRB **98**, 224421 (2018).

3. First-Principles Study on magnetic damping of Fe/MgO(001)

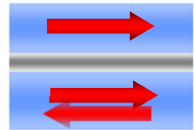
Y. Miura, in preparation

Thermal stability of magnetization in MTJs

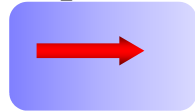
To achieve ultra high density MRAM

In-plane MTJ

Side view



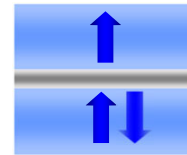
Top view



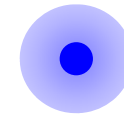
Aspect ratio >2

Perpendicular MTJ

Side view



Top view



For 10 year's
write endurance



Thermal stability factor

$$\frac{K_u V}{k_B T} \geq 60$$

K_u : uniaxial magnetic anisotropy

Large K_u is required with decreasing volume
towards scaling down of device dimensions

Examples of Perpendicular MTJ

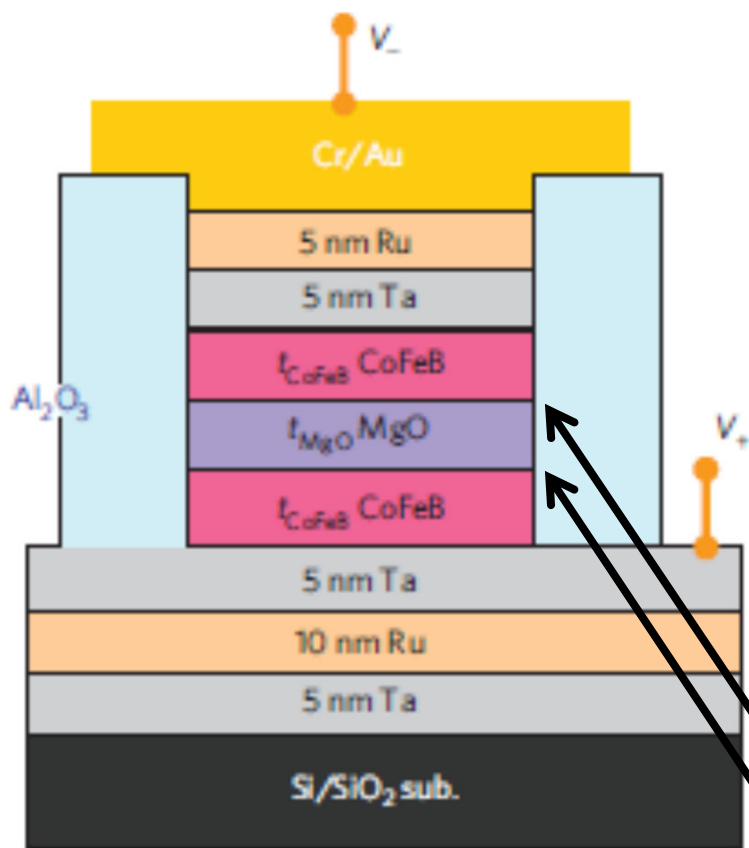
Using $L1_0$ -type FePt, CoPt, CoFePd alloys and its multilayered structures

- [1] M. Yoshikawa, *et al.*, IEEE Trans. Magn. vol.44 2573 (2008). (Toshiba)
- [2] K. Yakushiji, *et al.*, APEX vol. 3 053003 (2010). (AIST)
- [3] K. Mizunuma *et al.*, APEX vol. 4 023002 (2011). (Tohoku)

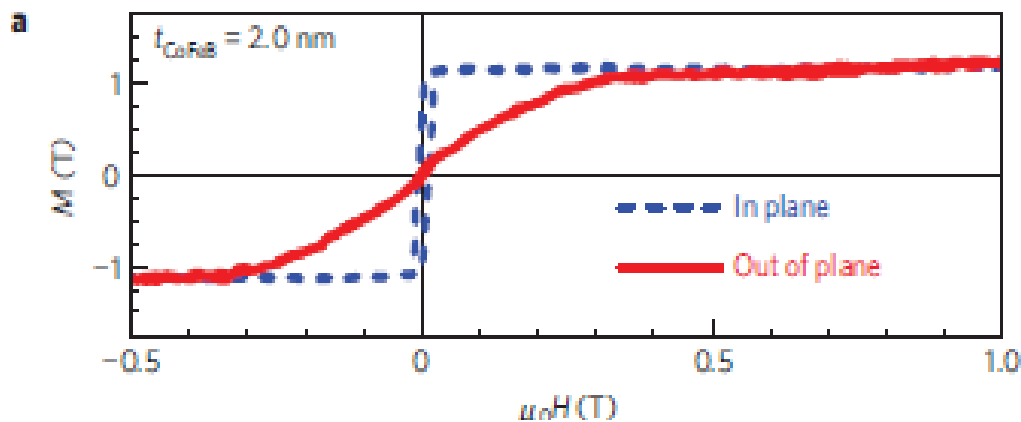
Interfacial Perpendicular Magnetic Anisotropy (PMA) for MgO

S. Ikeda, *et al.*, Nature Materials **9**, 721 (2010).

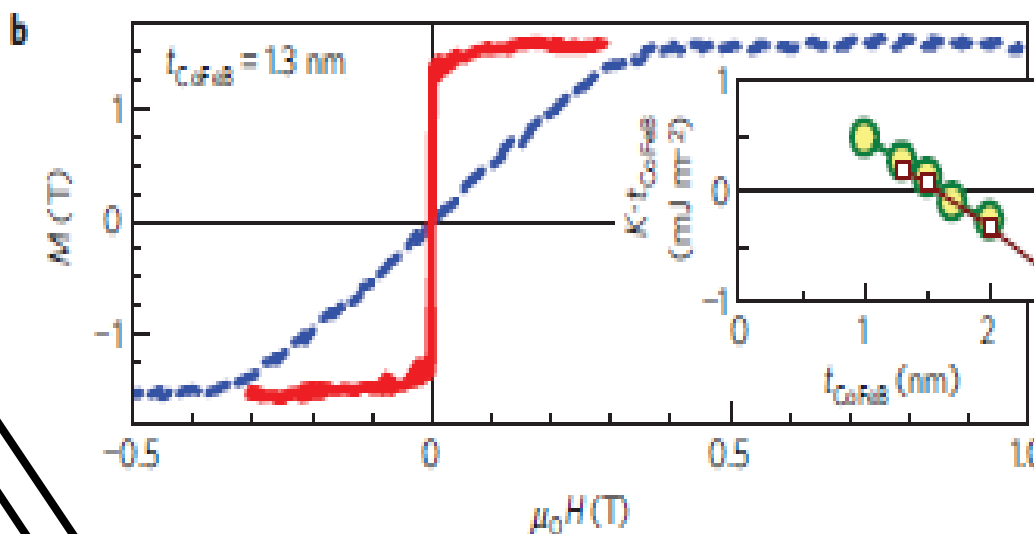
- CoFeB/MgO/CoFeB(001)



In-plane magnetization ($t_{\text{CoFeB}}=2.0\text{nm}$)



Perpendicular magnetization ($t_{\text{CoFeB}} < 1.3\text{nm}$)



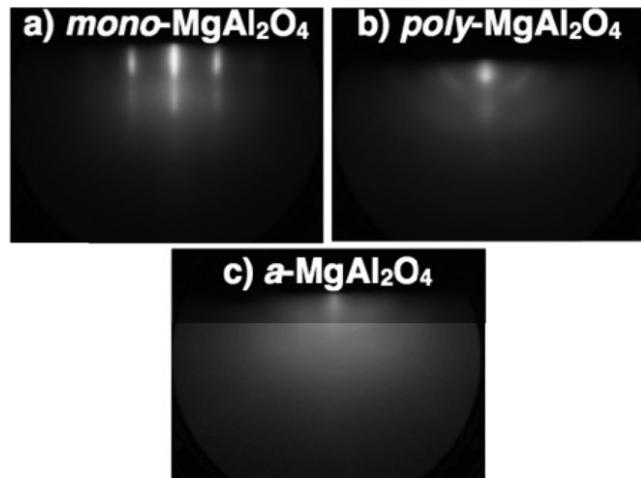
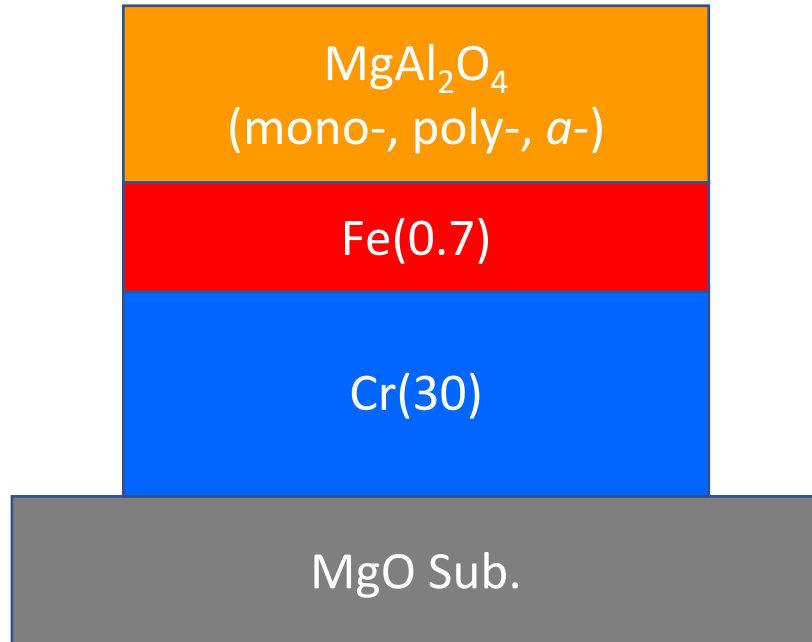
TMR ratio of 120% at 300K

Interfacial perpendicular MCA of Fe/MgO(001), which is $K_i=1.30\text{ mJ/m}^2$

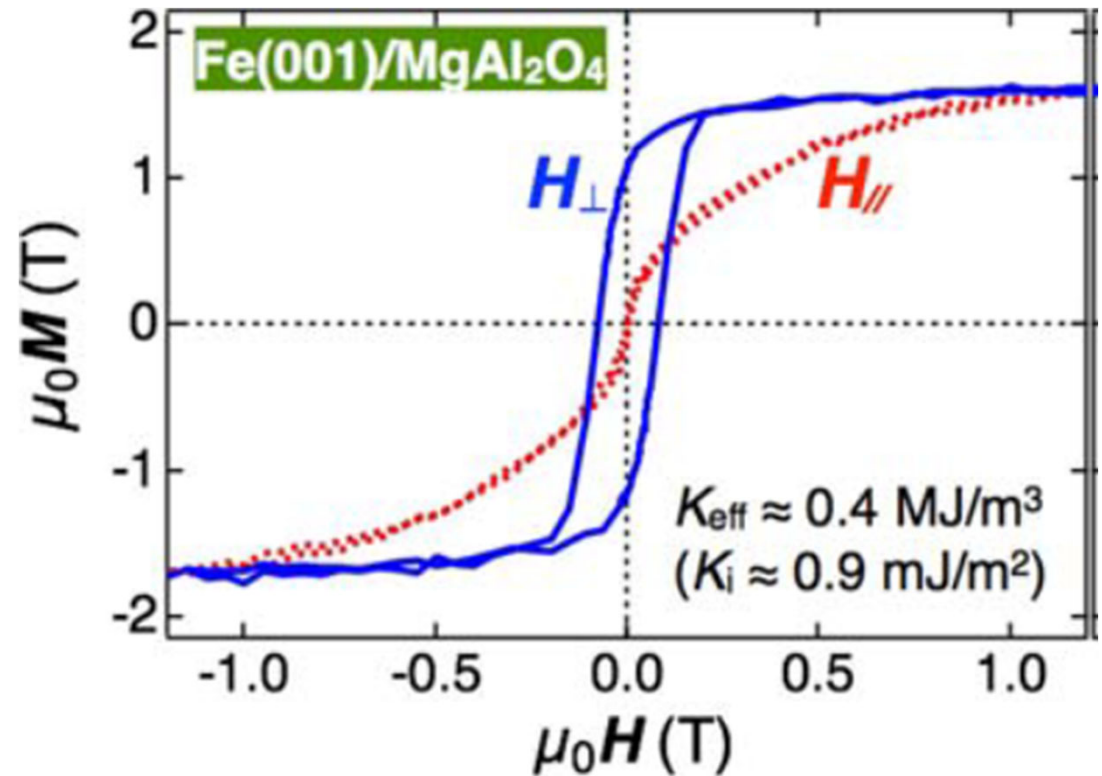
Interfacial Perpendicular Magnetic Anisotropy(PMA) for MgAl₂O₄(MAO)

Multilayer structure

Annealed @350-450°C



Lattice mismatch between
bcc-Fe and MgAl₂O₄ is 0.2%.



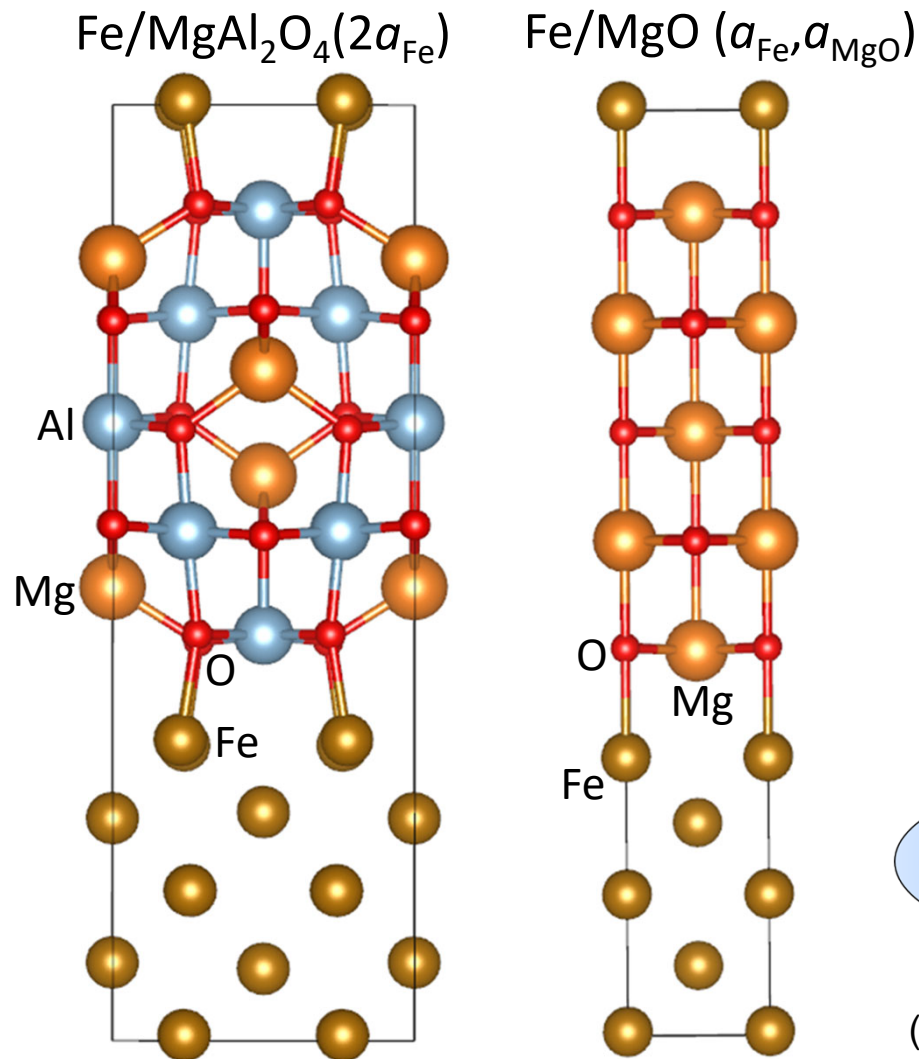
J. Koo, *et.al.*, Phys. status solidi RRL **8**, 841 (2014).

Ki of Fe/MgO(001) is 1.4mJ/m²,

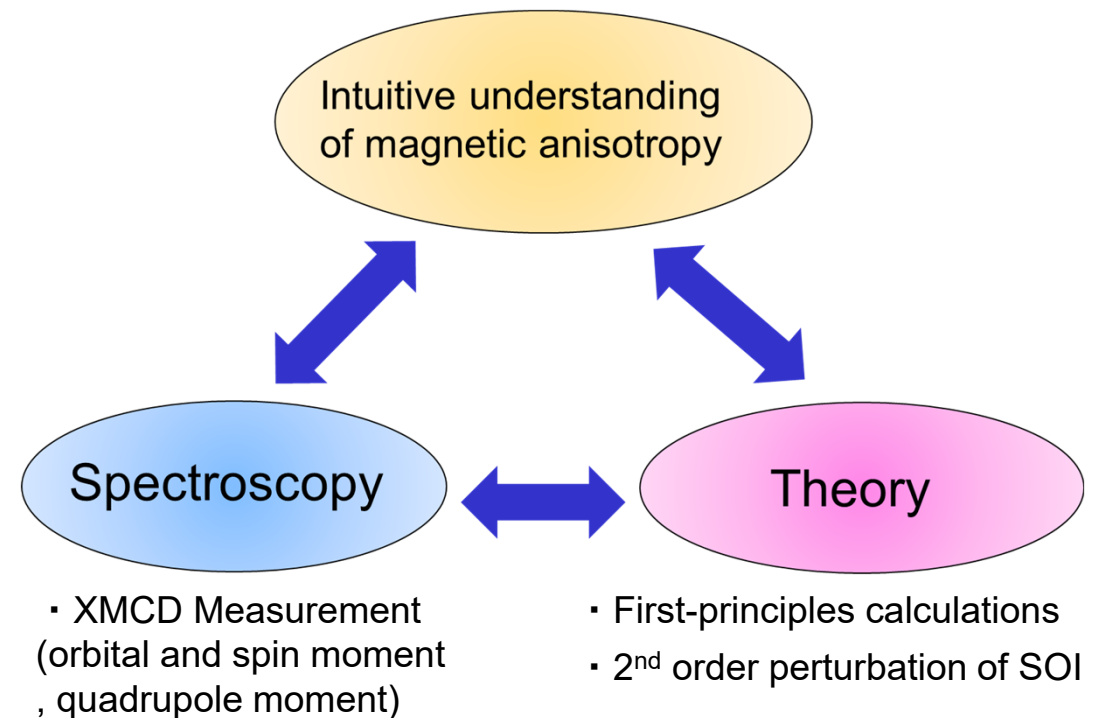
J. W. Koo, *et al.*, Appl. Phys. Lett. 103, 192401 (2013).

Purpose of this work

We study interfacial magnetocrystalline anisotropy (MAE) in Fe/MgAl₂O₄ and Fe/MgO by means of first-principles calculations based on density functional theory.



• origin of interfacial perpendicular magnetocrystalline anisotropy (PMA)



Second order perturbation of spin-orbit interaction (SOI)

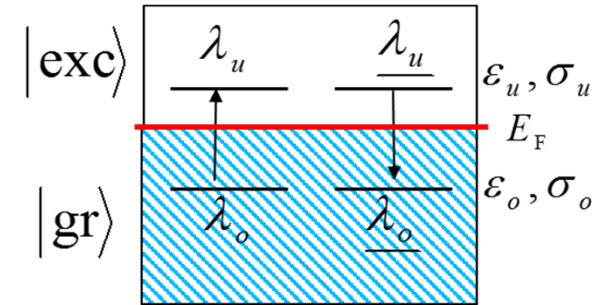
Bruno, PRB **39**, 865 (1989).

Wang, Wu, Freeman, PRB **47**, 14932 (1993).

van der Laan, JPCM **10**, 3239 (1998).

$$\delta E = - \sum_{\text{exc}} \frac{|\langle \text{exc} | H^{\text{SO}} | \text{gr} \rangle|^2}{\epsilon_{\text{exc}} - \epsilon_{\text{gr}}} \quad H^{\text{SO}} = \xi \vec{L} \cdot \vec{S}$$

$$|\text{gr}(\text{exc})\rangle = \sum_{\mu, \sigma} c_{i, \mu, \sigma} |i, \mu\rangle$$



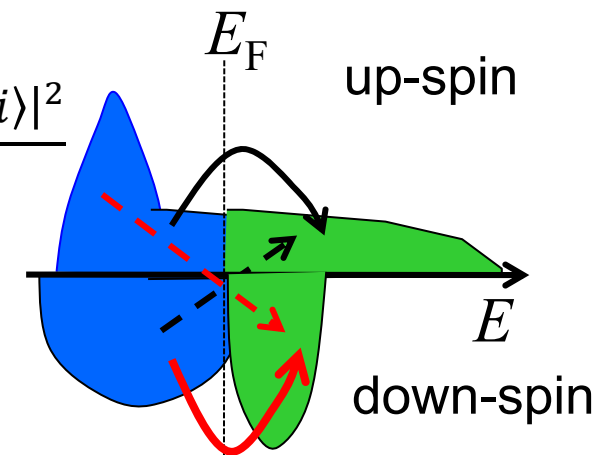
μ : local atomic orbital index
 i, j : index of atomic position

Magneto-crystalline anisotropy (MCA) energy

$$\Delta E^{\text{MCA}} = \delta E[\text{in-plane}] - \delta E[\text{perpendicular}]$$

$$\Delta E^{\text{MCA}}(i) = \sum_{\sigma, \sigma'} (-1)^{\delta_{\sigma' \sigma}} \xi_i^2 \sum_{o, u} \frac{|\langle o, \sigma' | L_z | u, \sigma, i \rangle|^2 - |\langle o, \sigma' | L_x | u, \sigma, i \rangle|^2}{\epsilon_{u, \sigma'} - \epsilon_{o, \sigma}}$$

$$= \underline{\Delta E_{\uparrow \Rightarrow \uparrow}^{\text{MCA}}(i)} + \underline{\Delta E_{\downarrow \Rightarrow \downarrow}^{\text{MCA}}(i)} + \underline{\Delta E_{\uparrow \Rightarrow \downarrow}^{\text{MCA}}(i)} + \underline{\Delta E_{\downarrow \Rightarrow \uparrow}^{\text{MCA}}(i)}$$



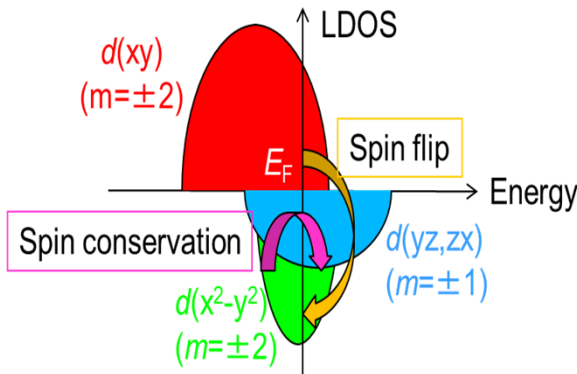
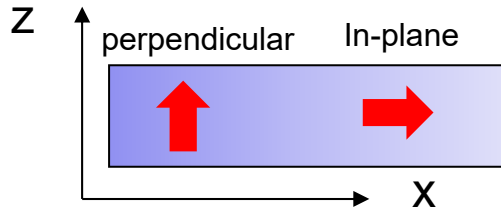
Orbital moment

$$\langle L^z \rangle = 4 \xi_i \sum_{o, u} \frac{|\langle o, \uparrow | L_z | u, \uparrow, i \rangle|^2 - |\langle o, \downarrow | L_z | u, \sigma, i \rangle|^2}{\epsilon_{u, \sigma'} - \epsilon_{o, \sigma}}$$

Spin conserving term and spin flip term in magnetic anisotropy

Spin conserving term

$$\Delta E_{\downarrow \Rightarrow \downarrow}^{\text{MCA}}(i) = \underbrace{+\xi_i^2 \sum_{o,u} \frac{|\langle u, \downarrow | L_z | o, \downarrow, i \rangle|^2}{\epsilon_{u,\downarrow} - \epsilon_{o,\downarrow}}}_{\text{red underline}} \underbrace{- \xi_i^2 \sum_{o,u} \frac{|\langle u, \downarrow | L_x | o, \downarrow, i \rangle|^2}{\epsilon_{u,\downarrow} - \epsilon_{o,\downarrow}}}_{\text{blue underline}}$$



$$L_z Y_l^m = m Y_l^m$$

Contributed to PMA energy, if there are d orbitals with the same magnetic quantum number m exist around E_F .

$$\langle zx, \downarrow | L_z | yz, \downarrow \rangle = 1$$

$$\langle x^2 - y^2, \downarrow | L_z | xy, \downarrow \rangle = 2$$

$$L_x Y_l^m \propto Y_l^{m\pm 1}$$

Contributed to PMA energy, if there are d orbitals with m and $m \pm 1$ exist around E_F .

$$\langle xy, \downarrow | L_x | zx, \downarrow \rangle = 1$$

$$\langle x^2 - y^2, \downarrow | L_x | zx, \downarrow \rangle = 1$$

$$\langle 3z^2 - r^2, \downarrow | L_x | yz, \downarrow \rangle = \sqrt{3}$$

Spin flip term

$$\Delta E_{\downarrow \Rightarrow \uparrow}^{\text{MCA}}(i) = \underbrace{-\xi_i^2 \sum_{o,u} \frac{|\langle u, \uparrow | L_z | o, \downarrow, i \rangle|^2}{\epsilon_{u,\uparrow} - \epsilon_{o,\downarrow}}}_{\text{red underline}} \underbrace{+ \xi_i^2 \sum_{o,u} \frac{|\langle u, \uparrow | L_x | o, \downarrow, i \rangle|^2}{\epsilon_{u,\uparrow} - \epsilon_{o,\downarrow}}}_{\text{blue underline}}$$

2nd order perturbation energy

$$\Delta E^{\text{MCA}} \approx \frac{\xi}{4\mu_B} (\Delta m^{\text{orb}}) + \frac{21}{2\mu_B} \frac{\xi^2}{\Delta E_{\text{ex}}} (m^T)$$

Orbital moment anisotropy term
⇒ Spin-conserving term

Magnetic dipole (Quadupole moment) term
⇒ Spin-flip term

Bruno, PRB **39**, 865 (1989).
Wang, Wu, Freeman, PRB **47**, 14932 (1993).
van der Laan, JPCM **10**, 3239 (1998).

Intuitive understanding of magneto-crystalline anisotropy (MCA)

P. Bruno, PRB **39**, 865 (1989).

G. Laan, JPCM **10**, 3239 (1998).

$$\Delta E^{\text{MCA}} \approx \frac{\xi}{4\mu_B} (\Delta m^{\text{orb}}) + \frac{21}{2\mu_B} \frac{\xi^2}{\Delta E_{\text{ex}}} (m^T)$$

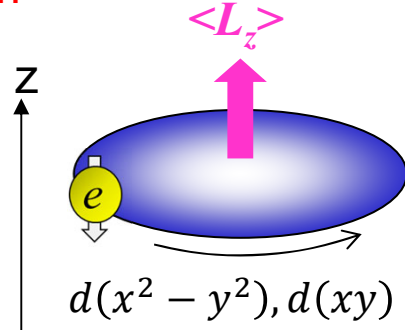
Orbital moment term Magnetic dipole term

$$\Delta m^{\text{orb}} = \langle L^z \rangle - \langle L^x \rangle$$

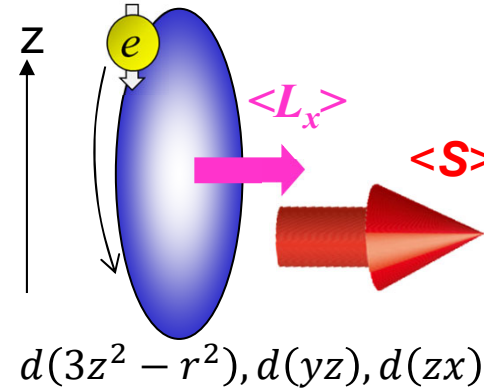
$$m^T = \langle T^z \rangle = -\langle Q^z S \rangle$$

Orbital moment term

$$H^{\text{SO}} = -\xi \vec{L} \cdot \vec{S}$$



Perpendicular magnetic anisotropy



In-plane magnetic anisotropy

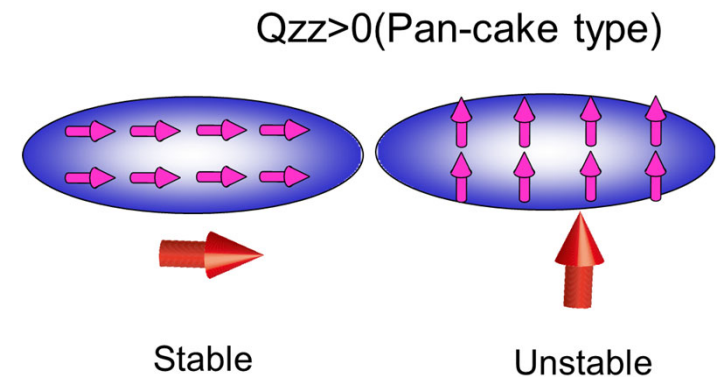
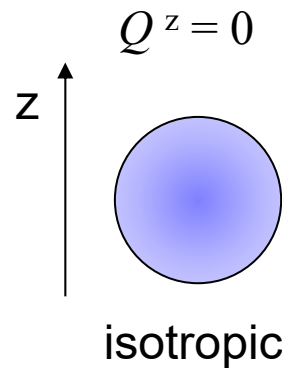
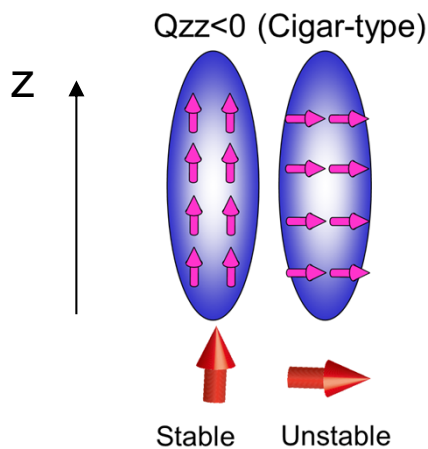
Magnetic dipole term $T \Rightarrow$ Quadrupole moment of spin density

$$\vec{T} \approx -\frac{2}{7} \mathbf{Q} \hat{S} \quad \rightarrow \quad T^z \approx -\frac{2}{7} \sum_{i=1}^5 Q_i^z S^i$$

Q: Quadrupole moment of spin density

$Q^z < 0$ ($T^z > 0$) \Rightarrow Prolate distribution

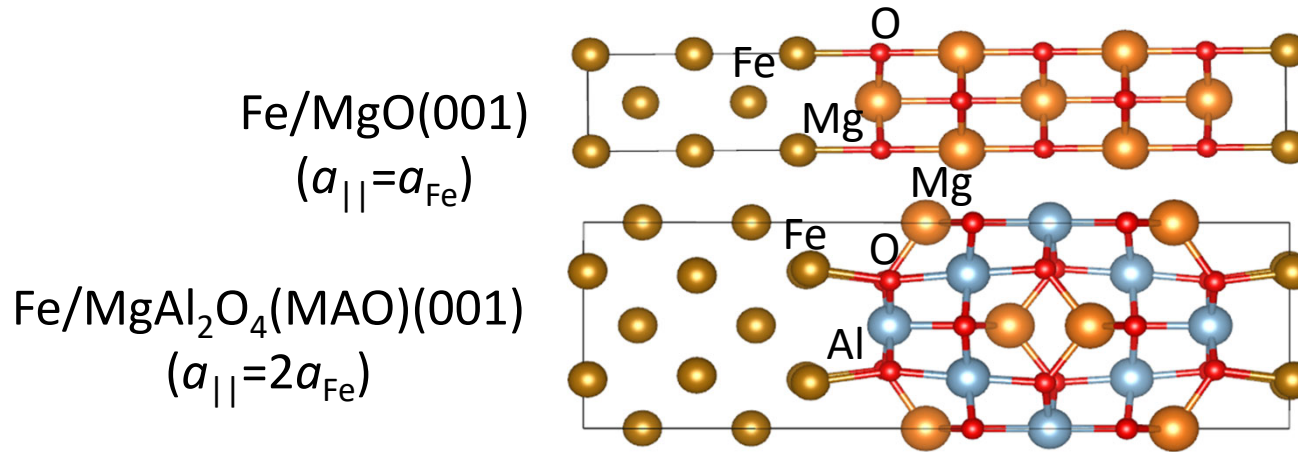
$Q^z > 0$ ($T^z < 0$) \Rightarrow Oblate distribution



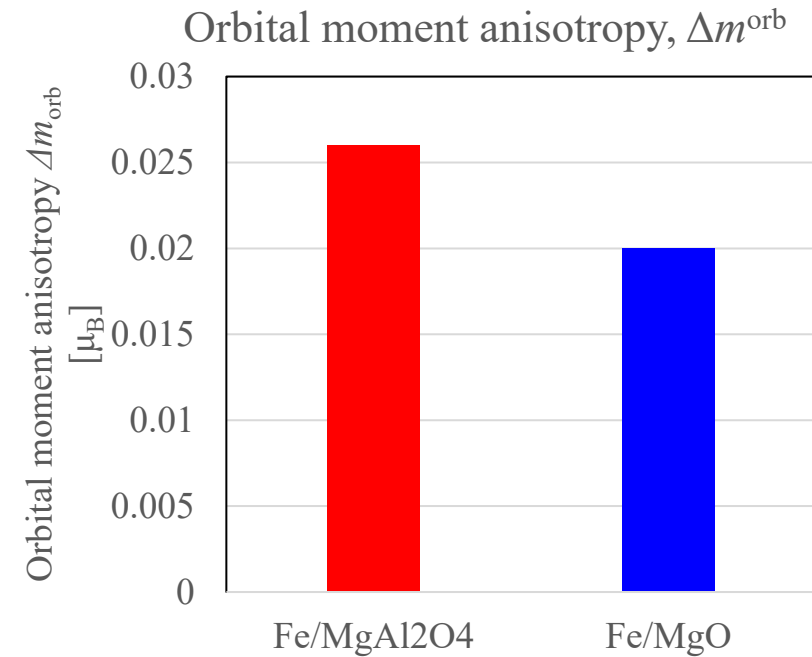
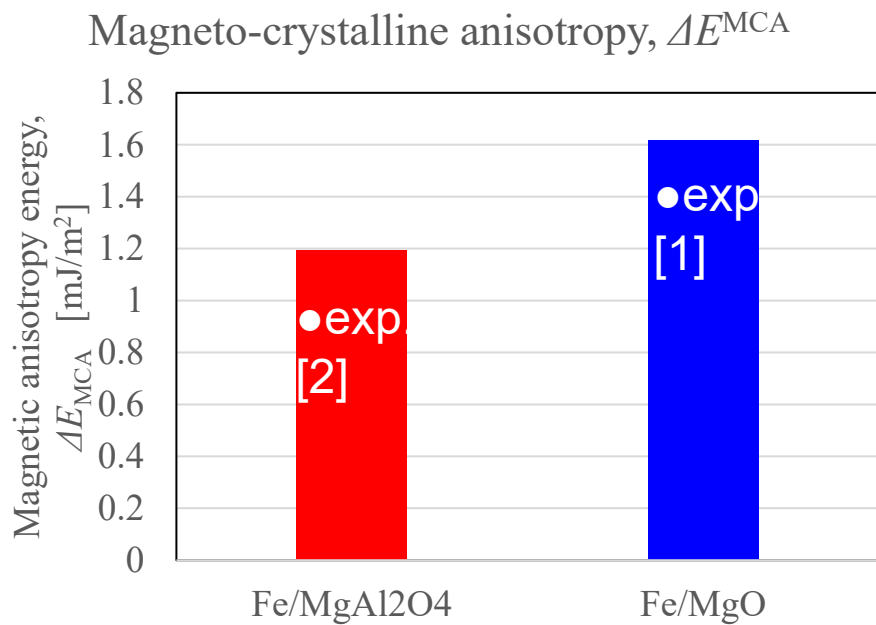
Perpendicular magnetic anisotropy

In-plane magnetic anisotropy

MCA energy for Fe/MgAl₂O₄(MAO) and Fe/MgO



K. Masuda and Y. Miura,
PRB **98**, 224421 (2018).



[1] J. W. Koo, *et al.*, Appl. Phys. Lett. 103, 192401 (2013).

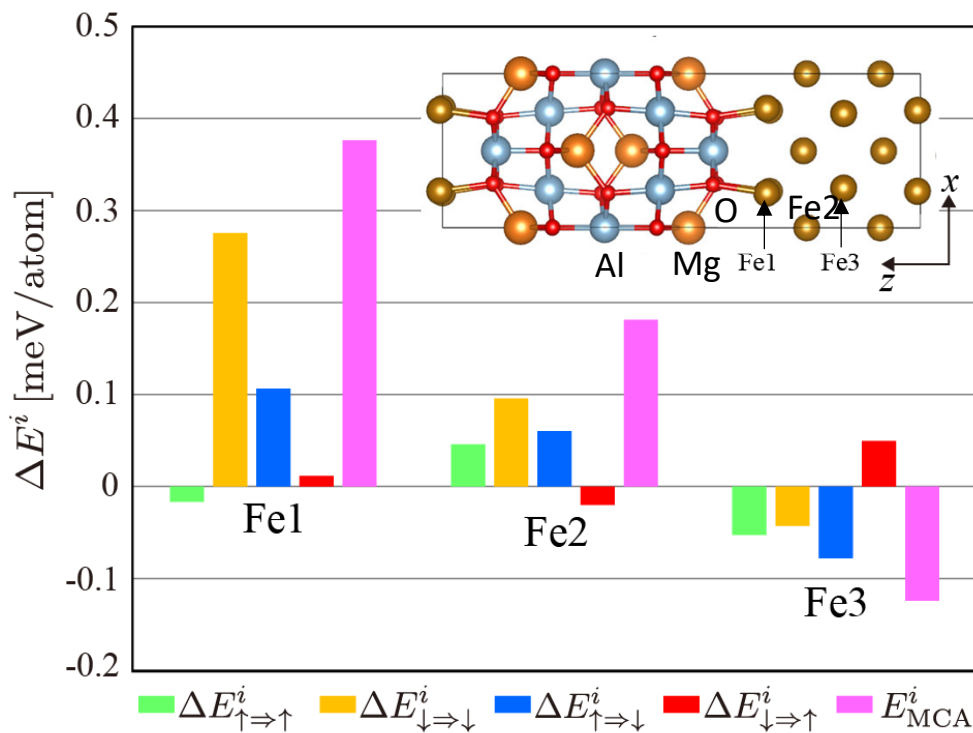
[2] J. W. Koo, *et al.*, Phys. status solidi RRL **8**, 841 (2014).

$$\Delta E^{MCA} \approx \frac{\xi}{4\mu_B} (\Delta m^{\text{orb}}) + \frac{21}{2\mu_B} \frac{\xi^2}{\Delta E_{\text{ex}}} (m^T)$$

Spin-decomposed PMA energy of Fe/MgAl₂O₄(MAO) and Fe/MgO

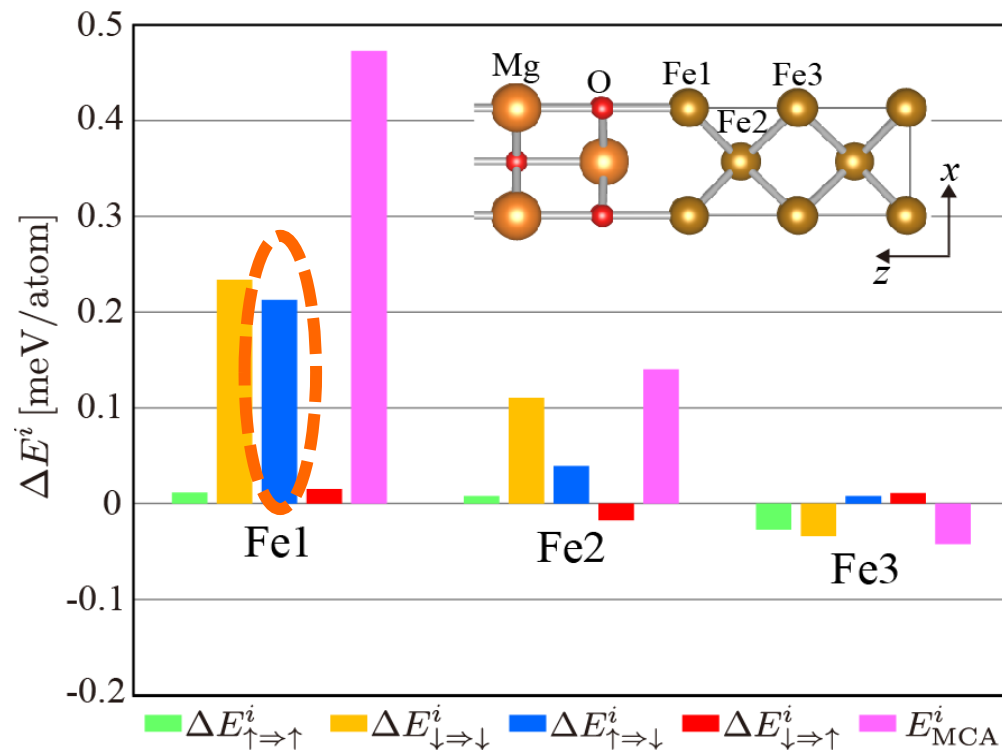
Fe/MgAl₂O₄(MAO) $a=a_{\text{Fe}}$

$\Delta E^{\text{MCA}}=1.2[\text{mJ/m}^2]$



Fe/MgO $a=a_{\text{Fe}}$

$\Delta E^{\text{MCA}}=1.6[\text{mJ/m}^2]$



- Interfacial Fe mainly contributes to Perpendicular (Positive) MCA
- Spin conservation term $\Delta E_{\downarrow \Rightarrow \downarrow}^{\text{MCA}}(i)$ mainly contributes to Perpendicular MCA.
- For Fe/MgO, the spin flip term $\Delta E_{\uparrow \Rightarrow \downarrow}^{\text{MCA}}(i)$ also contributes to Perpendicular MCA.

Magnetic dipole term of Fe/MgAl₂O₄ and Fe/MgO

$$m^T = T^z \approx -\frac{2}{7}(-16m^{3z^2-r^2} - 8m^{zx} - 8m^{yz} + 16m^{xy} + 16m^{x^2-y^2})$$

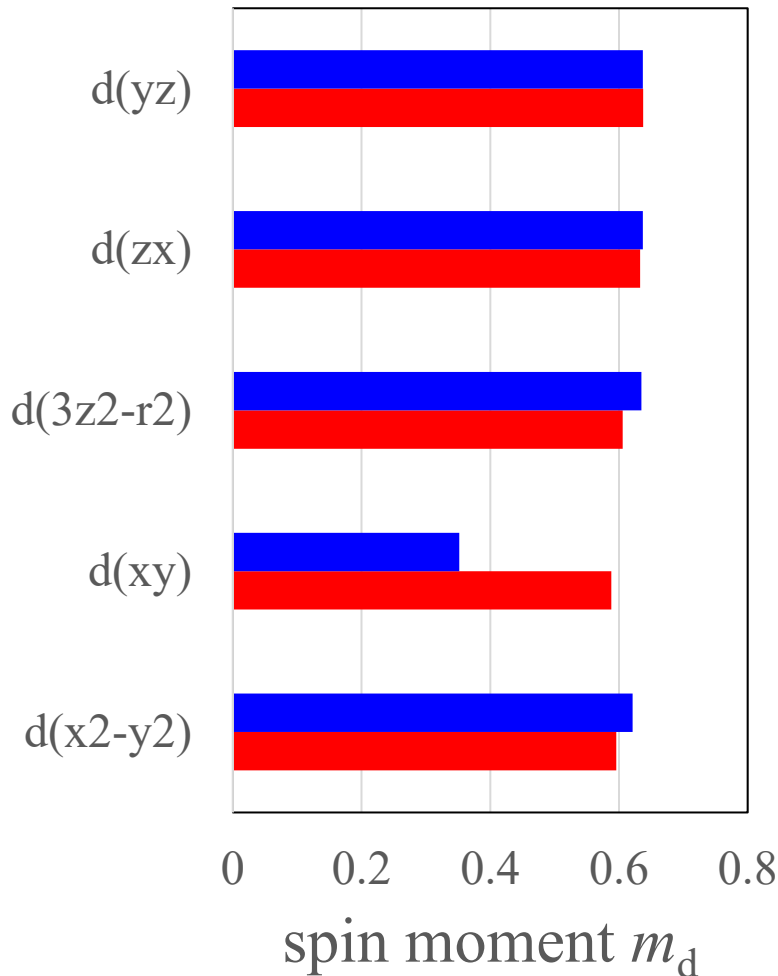
J. Stöhr and H. König, PRL **75**, 3748 (1995).

Quadrupole distribution of *d* orbitals

Orbital <i>i</i>	$\alpha = x, y \text{ or } z$ $4(7Q_\alpha^i)$
<i>d_{yz}</i>	
<i>d_{xz}</i>	
<i>d_{3z^2-r^2}</i>	
<i>d_{xy}</i>	
<i>d_{x^2-y^2}</i>	

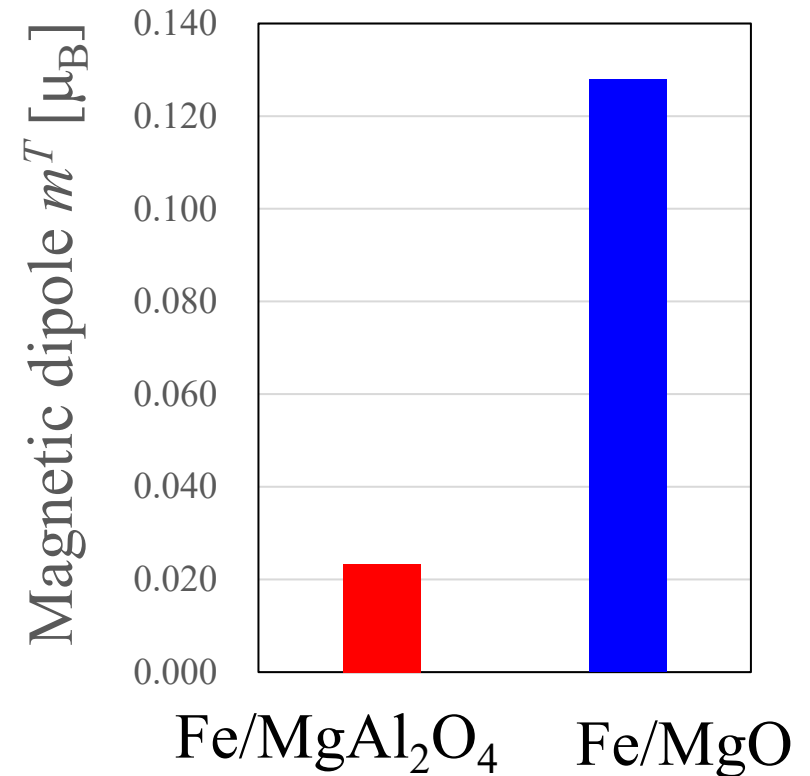
Spin moment of each *d* orbital for interfacial Fe

■ Fe/MgO ■ Fe/MgAl₂O₄



$$m^T = \langle T^z \rangle = -\langle Q^z S \rangle$$

Magnetic dipole term, m^T

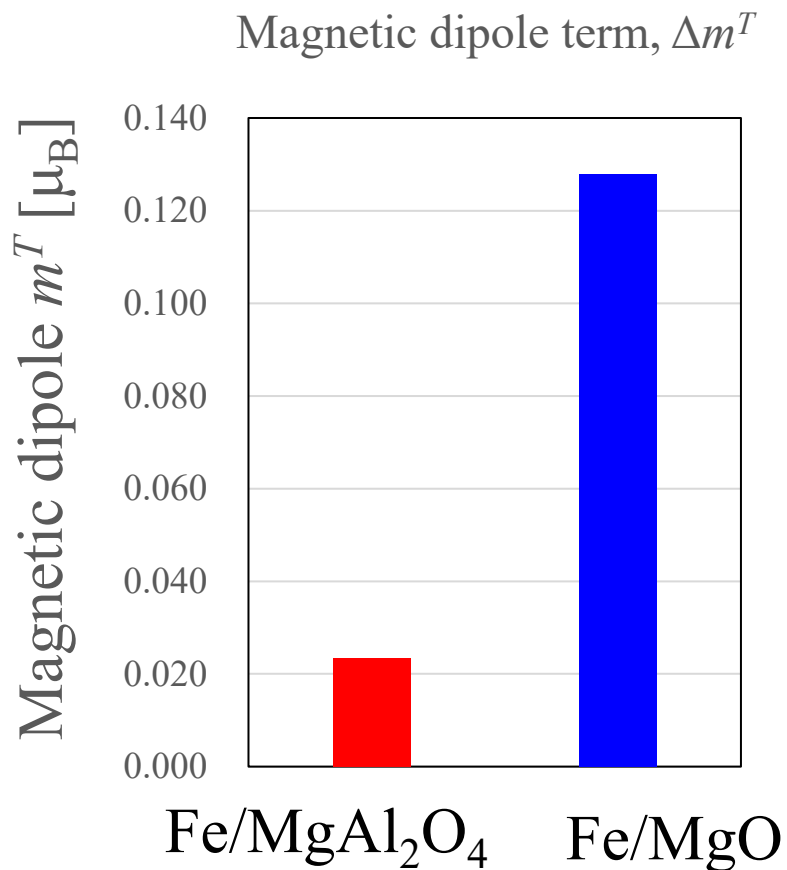


Magnetic dipole term of Fe/MgAl₂O₄ and Fe/MgO

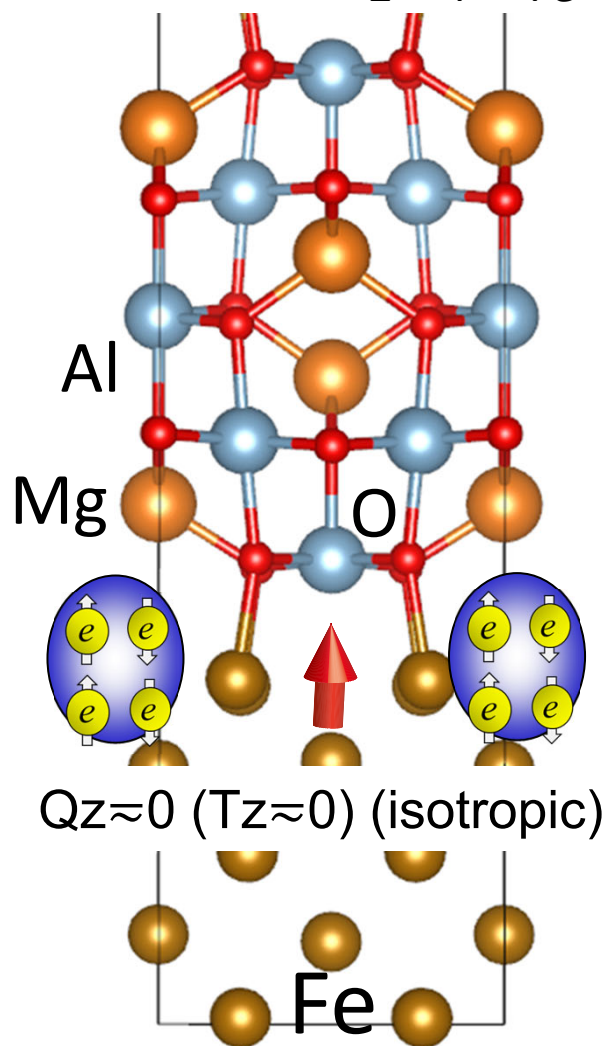
$$\langle T^z \rangle \approx -\frac{2}{7} \sum_{i=1}^5 Q_i^z S^i = -\frac{2}{7} (-16m^{3z^2-r^2} - 8m^{zx} - 8m^{yz} + 16m^{xy} + 16m^{x^2-y^2})/16$$

J. Stöhr and H. König, PRL **75**, 3748 (1995).

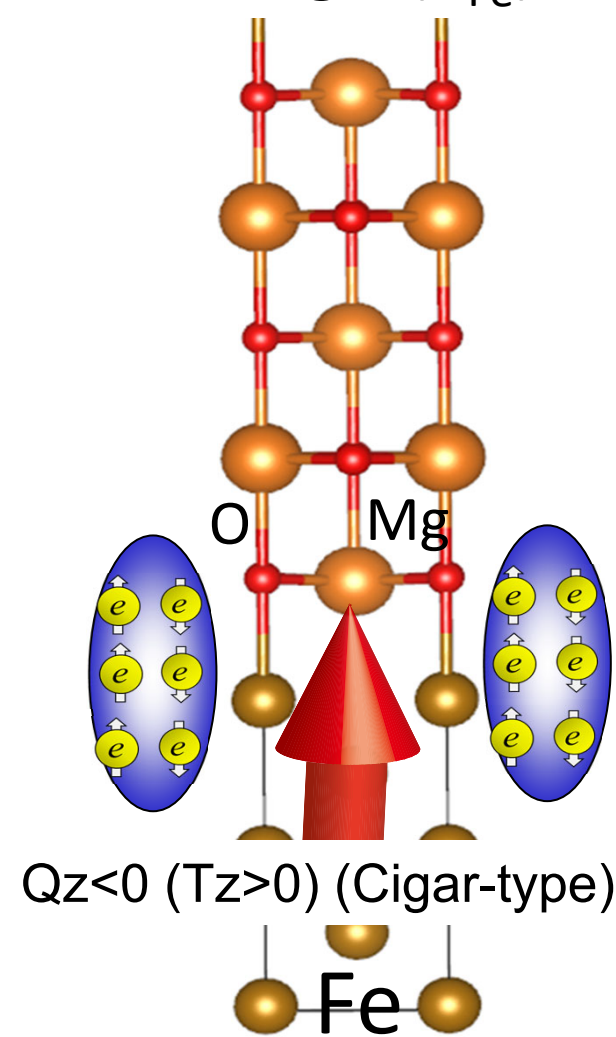
$$m^T = \langle T^z \rangle = -\langle Q^z S \rangle$$



Fe/MgAl₂O₄ (a_{Fe})



Fe/MgO (a_{Fe})



Summary of the second topic

- Fe/MgAl₂O₄(001) show **Perpendicular MCA**, which is slightly **smaller than that of Fe/MgO(001)**.
- For Fe/MgO(001), **not only spin conservation term $\Delta E_{\downarrow \Rightarrow \downarrow}$ but also spin-flip term $\Delta E_{\uparrow \Rightarrow \downarrow}$ contributes to Perpendicular MCA**, resulting in larger MCA energy than that of Fe/MgAl₂O₄.
- **Cigar type quadrupole moment additionally increases the Perpendicular MCA of Fe/MgO**, but not for Fe/MgAl₂O₄(MAO).



The quadrupole moment of spin-density is essential to understand the magneto-crystalline anisotropy (MCA) especially for ferromagnetic interfaces.

Topics

0. Introduction on spintronics

1. Spin-dependent transport in magnetic tunnel junctions with half-metallic Heusler alloys

Y. Miura, *et al.*, PRB **83**, 214411 (2011).

2. Magneto-crystalline anisotropy at interfaces of Fe(001) with MgO and MgAl₂O₄

K. Masuda and Y. Miura, PRB **98**, 224421 (2018).

3. **First-Principles Study on magnetic damping of Fe/MgO(001)**

Y. Miura, in preparation

Voltage-driven dynamic switching in MTJ

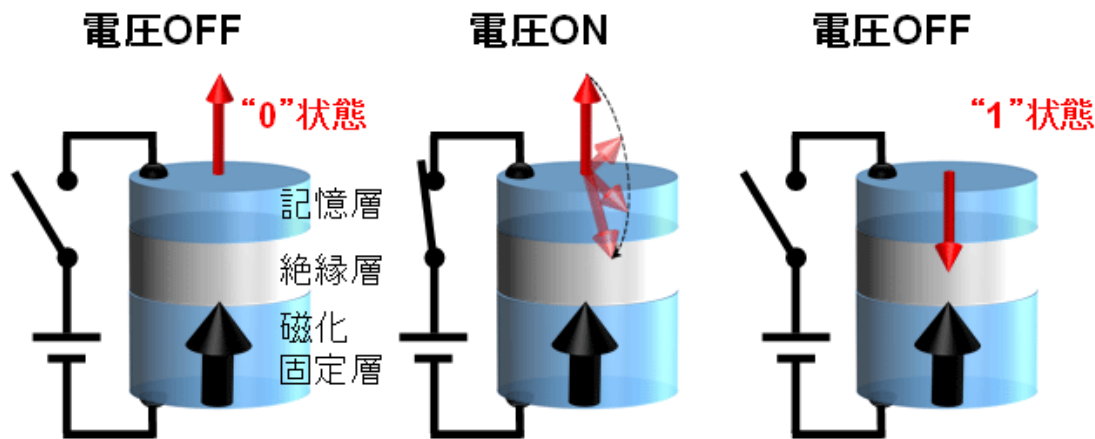
Applied Physics Express 9, 013001 (2016)

<http://doi.org/10.7567/APEX.9.013001>



Evaluation of write error rate for voltage-driven dynamic magnetization switching in magnetic tunnel junctions with perpendicular magnetization

Yoichi Shiota*, Takayuki Nozaki, Shingo Tamaru, Kay Yakushiji, Hitoshi Kubota, Akio Fukushima, Shinji Yuasa, and Yoshishige Suzuki

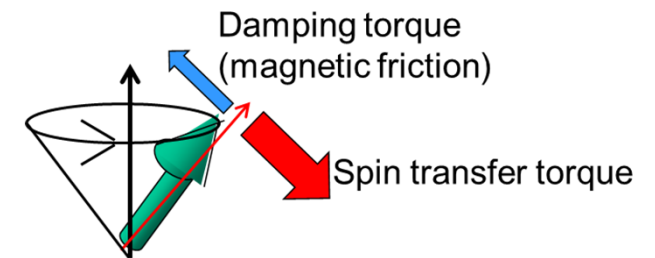


From website of Sahashi's ImPACT project in JST

Pulsed bias voltage changes PMA of interface of FM layer and promote the precession motion of the magnetization.

➡ By removing the voltage with a proper pulse duration, such as a half precession period, magnetization switching can be achieved.

➡ Basically, no current flow



Write Error Rate (WER)

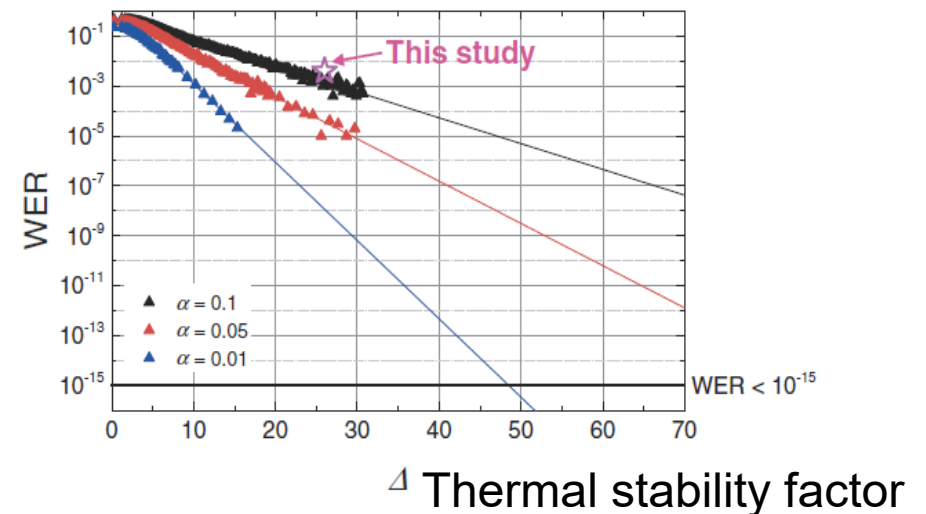


Fig. 4. Calculated WER as a function of Δ for fixed tilted magnetization angle and half precession period τ_{pulse} for various damping constants.

Large K_u and Small damping α can reduce the WER

Experiments electric field effects of PMA and magnetic damping

APPLIED PHYSICS LETTERS **105**, 052415 (2014)



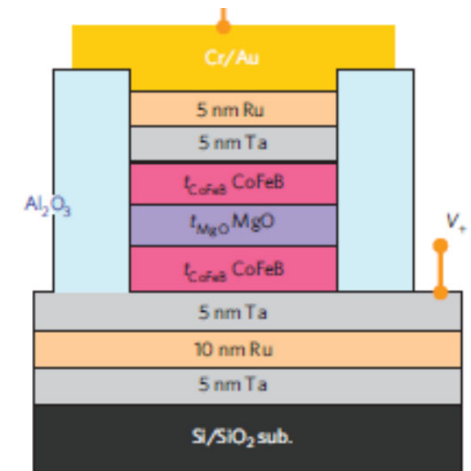
Electric-field effects on magnetic anisotropy and damping constant in Ta/CoFeB/MgO investigated by ferromagnetic resonance

A. Okada,¹ S. Kanai,¹ M. Yamanouchi,^{1,2} S. Ikeda,^{1,2} F. Matsukura,^{3,2,a)} and H. Ohno^{1,2,3}

¹Laboratory for Nanoelectronics and Spintronics, Research Institute of Electrical Communication, Tohoku University, 2-1-1 Katahira, Aoba-ku, Sendai 980-8577, Japan

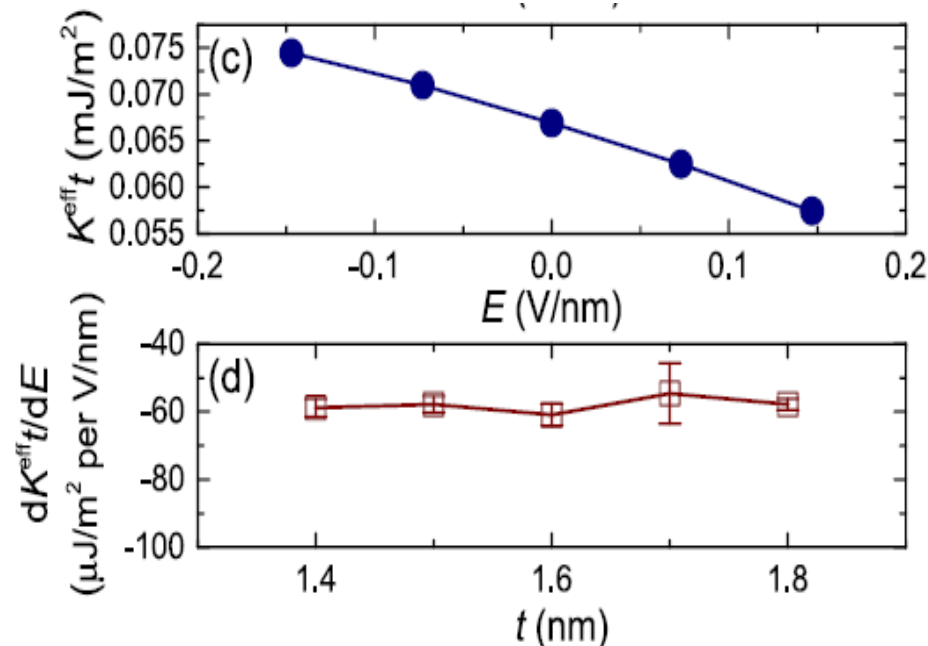
²Center for Spintronics Integrated Systems, Tohoku University, 2-1-1 Katahira, Aoba-ku, Sendai 980-8577, Japan

³WPI-Advanced Institute for Materials Research (WPI-AIMR), Tohoku University, 2-1-1 Katahira, Aoba-ku, Sendai 980-8577, Japan



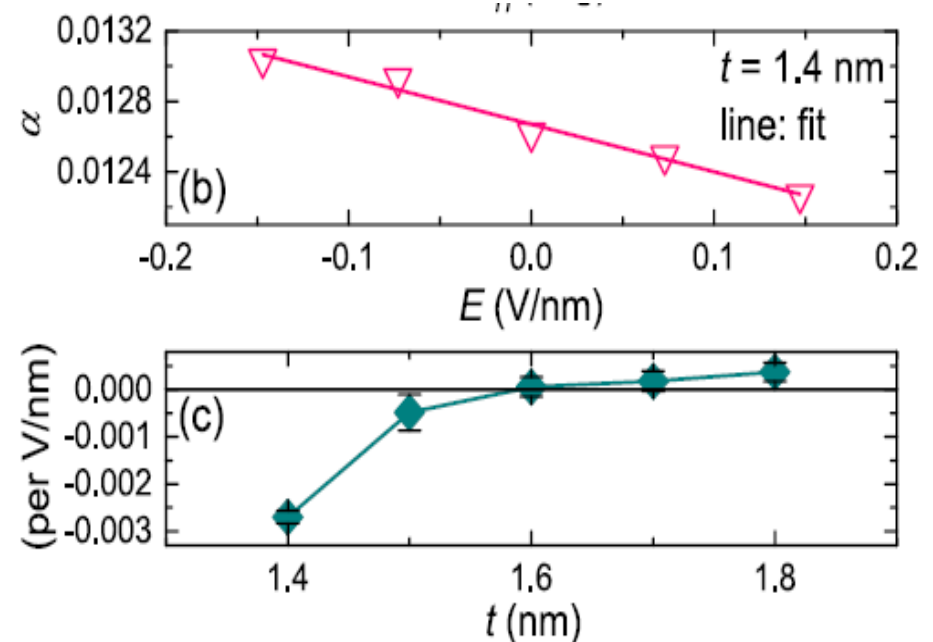
-21% of magnetic damping α is changed by 1V/nm EF for $t=1.4$ nm

Magnetic anisotropy change by EF



EF dependence is insensitive to thickness of FM layer

Magnetic damping change by EF

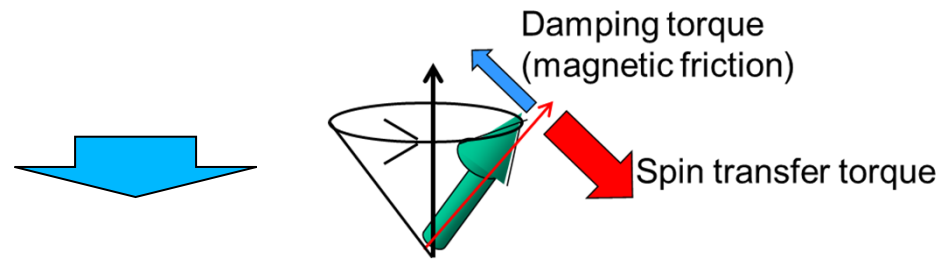


Large thickness dependence of FM layer

Purpose of this work

If PMA and magnetic damping can be simultaneously reduced by applied voltage, we can drastically reduce power consumption and write error rate in magnetization reversal of MRAM.

Voltage dependence of magnetic damping is hardly investigated.



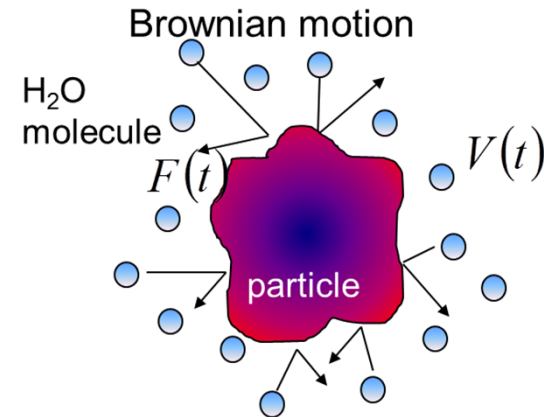
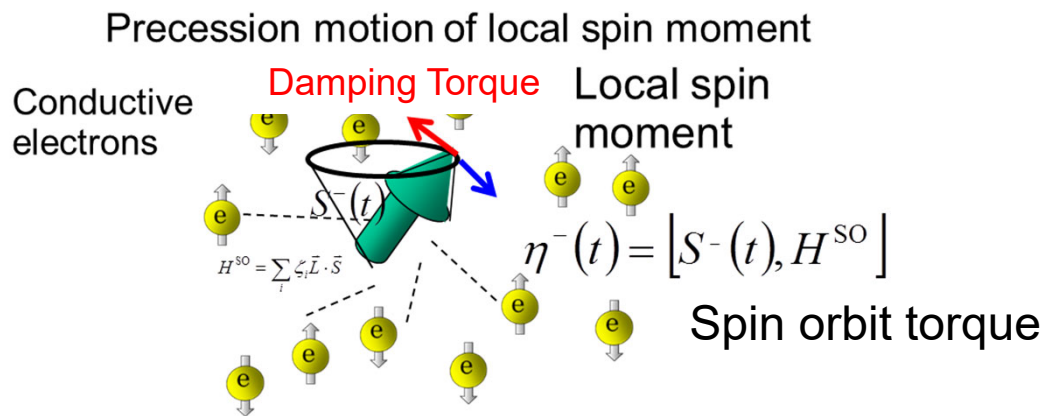
This work investigates the voltage dependence of magnetic damping and magnetic anisotropy of Fe/MgO interface based on the first-principles calculation.

Origin of Magnetic Damping α

- Electronic system
- Phonon
- Atomic disorder
- Other extrinsic factors

Kambersky's torque correlation model

V. Kambersky, Czechoslovak Journal of Physics B **26**, 1366 (1976).



Generalized Langevin equation for magnetization dynamics

$$\frac{dS^-(t)}{dt} = \underbrace{-i\Omega S^-(t)}_{\text{Precession-term}} - \underbrace{i\eta^-(t)}_{\text{Spin-torque term from SOI}} - \underbrace{\int_0^t P^{-1} \langle [\eta^-(t'), \eta^+] \rangle_0 S^-(t) dt'}_{\text{Damping-term}}$$

Magnetic susceptibility

$$\chi^+(\omega) = -\frac{\mu_0 (g\mu_B)^2}{\hbar V} \frac{P}{\omega + i0 - (\Omega - \Delta) - P^{-1} F(\omega + i0)}$$

Green function of Torque operator

$$F(\omega + i0) = -i \int_{-\infty}^{\infty} \langle [\eta^-(t), \eta^+] \rangle_0 \theta(t) e^{i(\omega+i0)t} dt$$

Magnetic susceptibility from LLG equation

$$\chi^+(\omega) = -\frac{\gamma M_s}{\omega - \gamma H_{eff} + i\alpha\omega}$$

Magnetic damping constant (comparing macroscopic formula)

$$\alpha = -\lim_{\omega \rightarrow 0} \frac{\gamma}{\hbar \mu_0 V M_s} \text{Im} \left[\frac{1}{\omega} F(\omega + i0) \right]$$

First-principles calculation of damping constant

V. Kambersky, Czechoslovak Journal of Physics B **26**, 1366 (1976).

$$\alpha = \frac{g^2 \mu_0 \mu_B^2}{\pi \hbar V \gamma M_S} \sum_{\vec{k}} \sum_{nm} \left| \Gamma_{nm}^-(\vec{k}) \right|^2 \frac{\delta}{(E_F - E_{n\vec{k}})^2 + \delta^2} \frac{\delta}{(E_F - E_{m\vec{k}})^2 + \delta^2}$$

$$\gamma = \mu_0 g \mu_B / \hbar$$

Matrix elements of torque operator

$$\Gamma_{nm}^-(\vec{k}) = \langle n, \vec{k} | \zeta [S^-, H^{SO}] | m, \vec{k} \rangle$$

Eigenstates at each
k-point and band

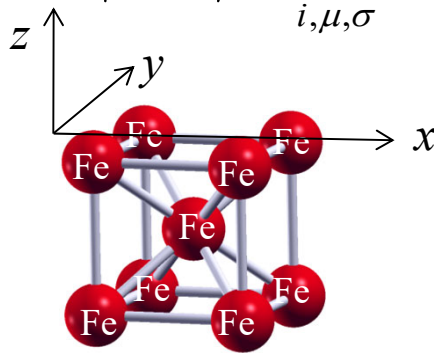
$$H_{SO} = \xi \vec{L} \cdot \vec{S} \quad \text{Spin-orbit interaction}$$

$$|m, \vec{k}\rangle = \sum_{i, \mu, \sigma} c_{i\mu}^{\vec{k}m\sigma} |i\mu\rangle$$

matrix elements of torque operator
based on the local atomic orbital

VASP code

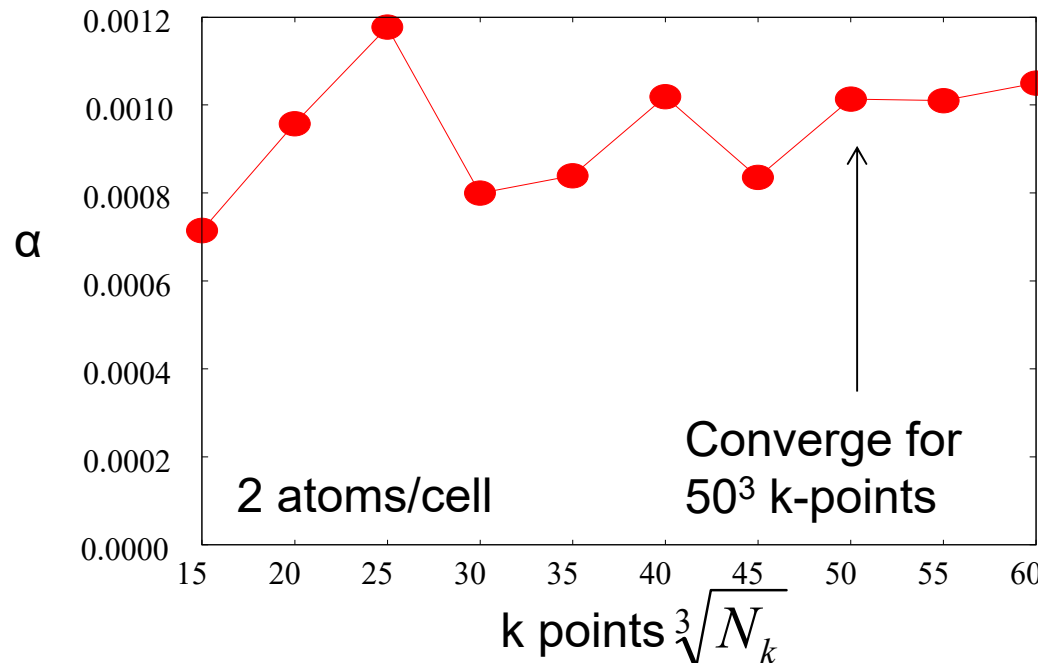
Bulk-Fe



$\alpha=0.0011$ (this work)

$\alpha=0.0013$ (by Gilmore)

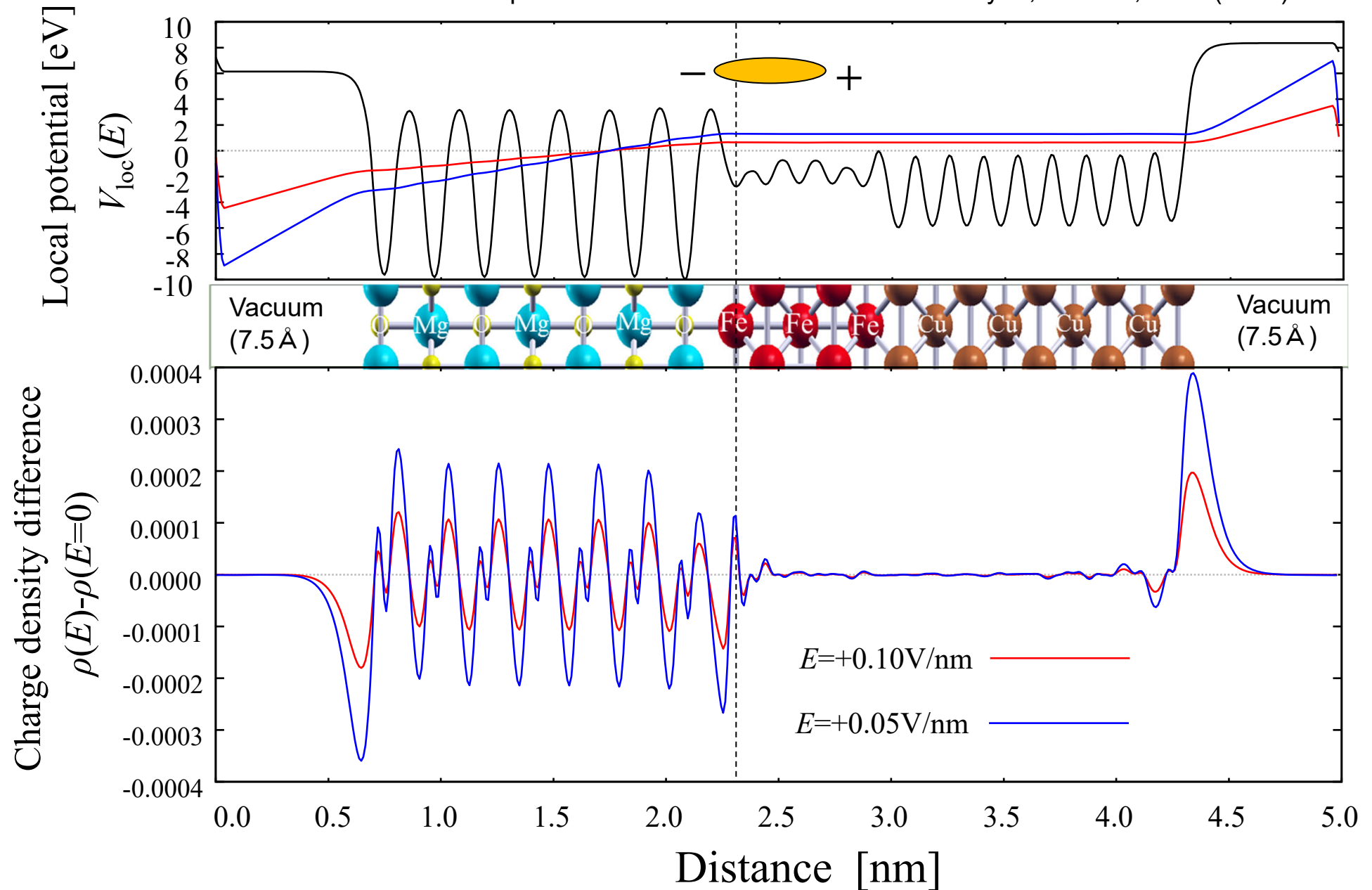
K. Gilmore, PRL **99**, 027204 (2007)



\Rightarrow For Fe/MgO(001) interface, I considered 50x50 k-points.

Potential and charge for model system

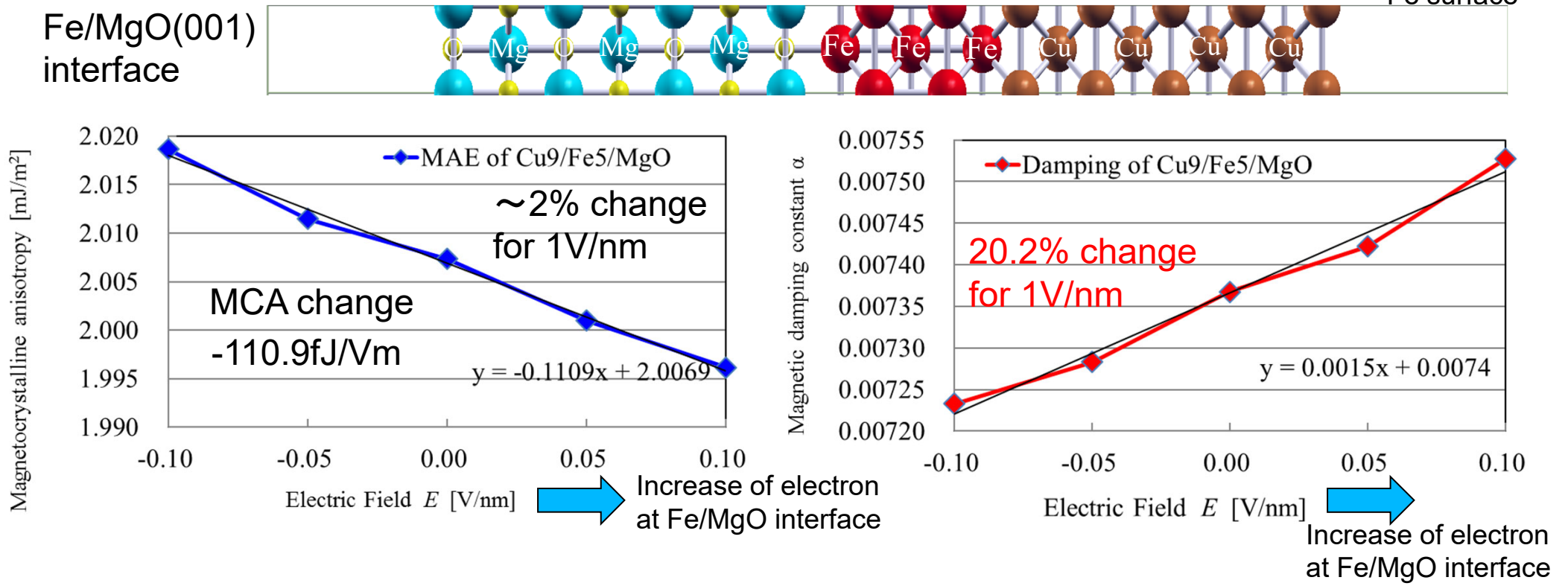
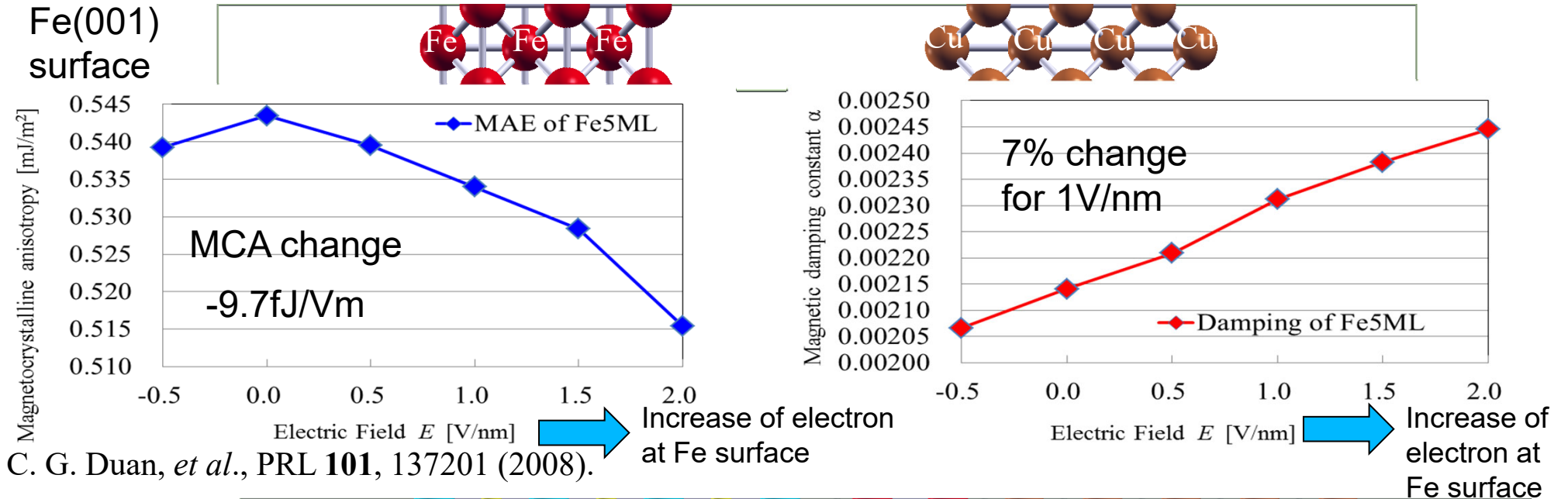
Dipole correction \Rightarrow G. Makov and M. C. Payne, PRB **51**, 4014 (1995).



$E > 0$: Increase of electron accumulation at Fe/MgO interface

$E < 0$: Decrease of electron accumulation at Fe/MgO interface

Voltage dependence of MCA and damping α of Fe surface and Fe/MgO interface



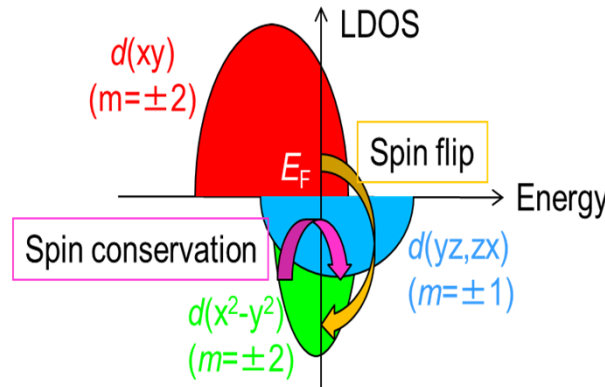
Decomposition of magnetic damping α

Torque operator $\Gamma^- = [S^-, H^{SO}] = \zeta (S^z L^- - S^- L^z)$

Spin conservation (Orbital deexcitation) term

$$\langle u^\sigma | L^- | o^\sigma \rangle$$

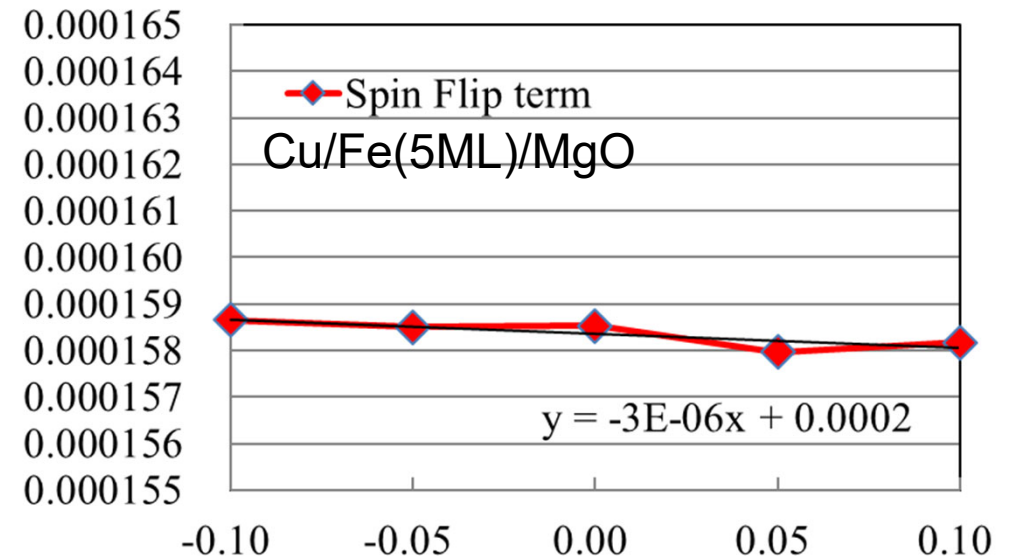
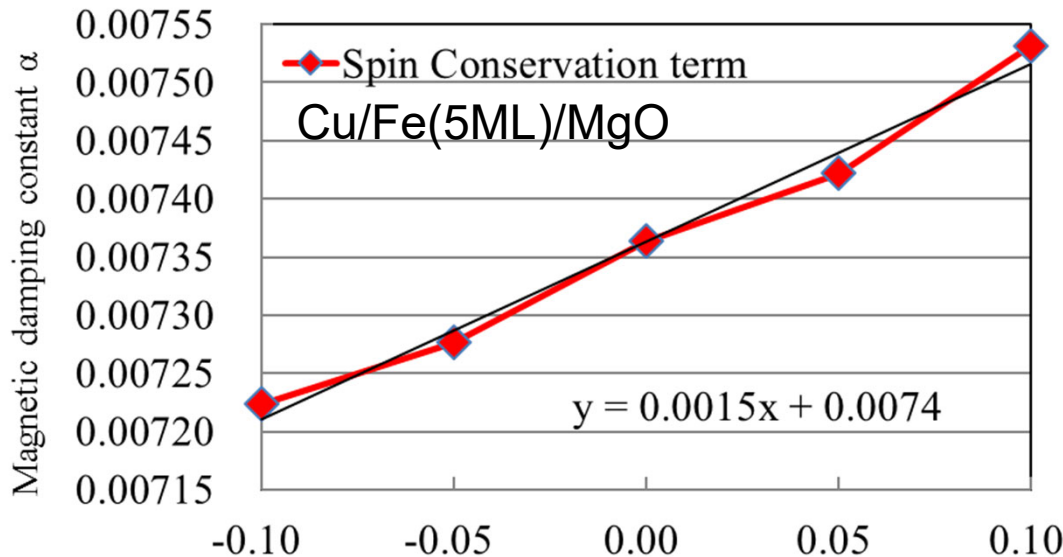
The matrix elements are non-zero for atomic orbitals between different magnetic quantum number, such as $d(yz, zx) - d(z^2)$, $d(yz, zx) - d(x^2 - y^2)$, $d(yz, zx) - d(xy)$



Spin flip (Orbital conservation) term

$$\langle u^{-\sigma} | L_z | o^\sigma \rangle$$

The matrix elements are non-zero for atomic orbitals between same magnetic quantum number, such as $d(yz) - d(zx)$, $d(x^2 - y^2) - d(xy)$

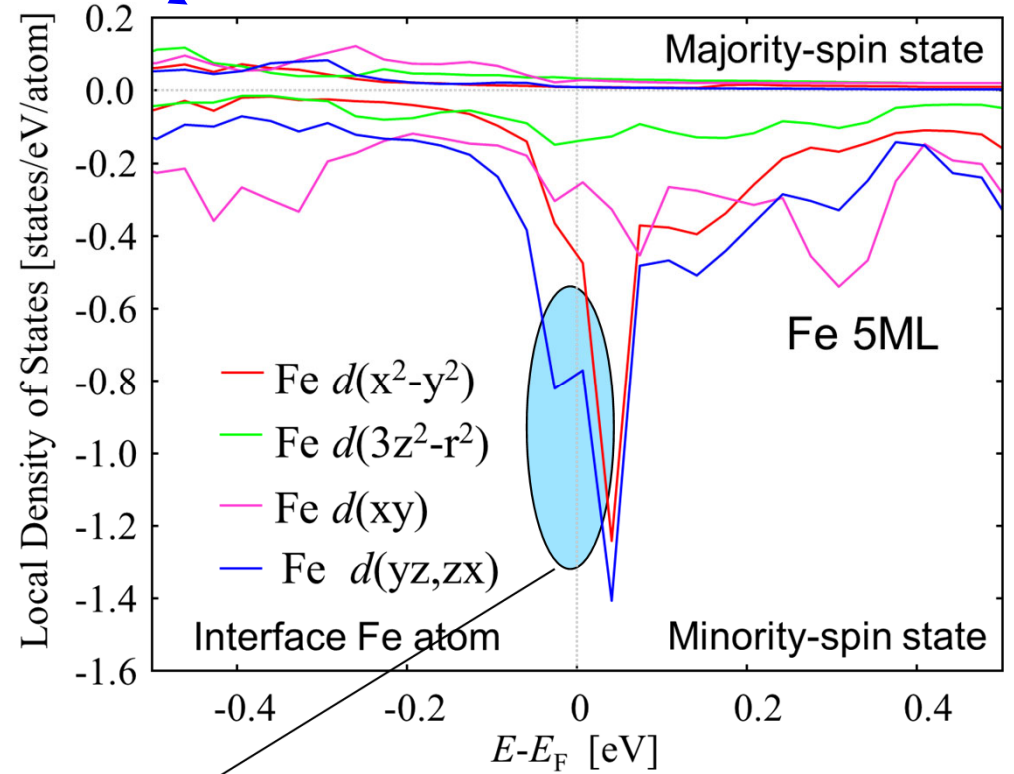
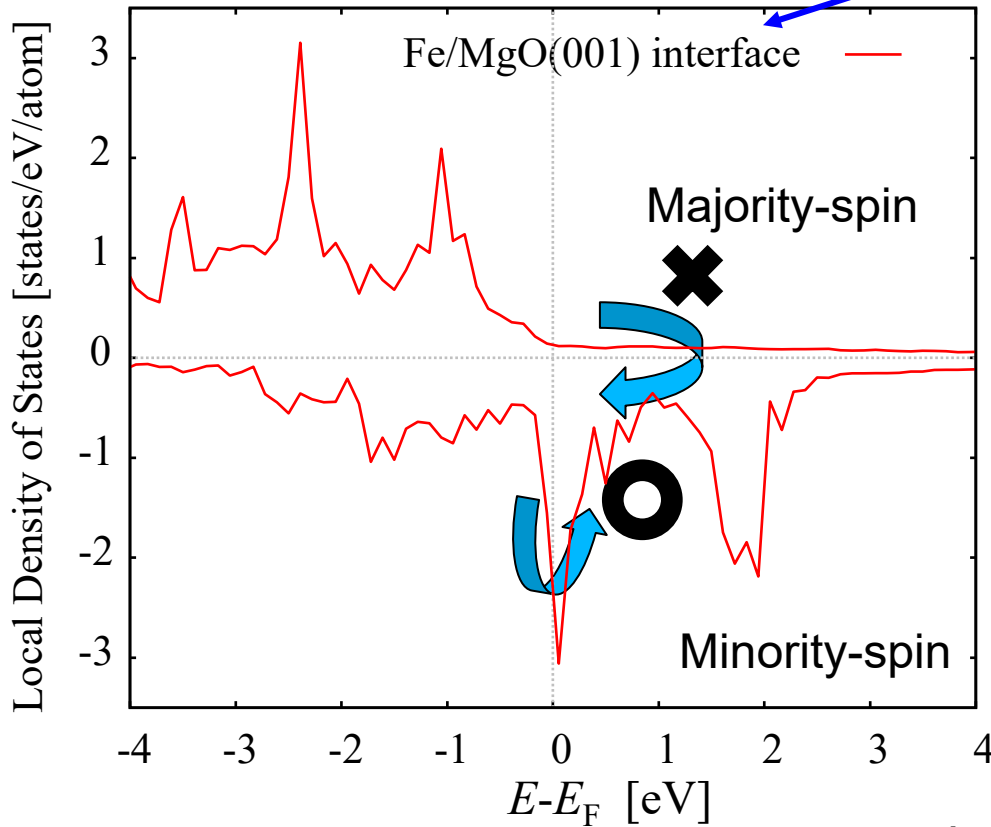
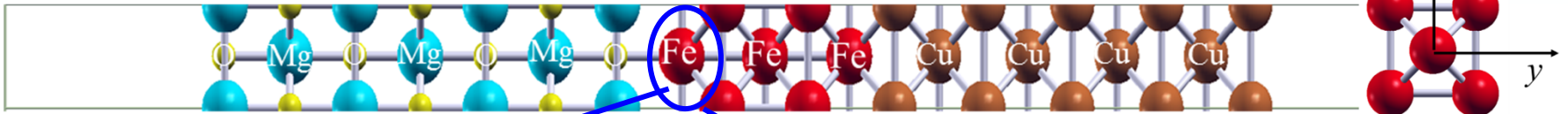


Electric Field E [V/nm] \rightarrow Increase of electron at Fe/MgO interface

Electric Field E [V/nm]

Origin of electric field dependence

Fe/MgO(001) interface



Second order perturbation of SOI

D. Wang, et al., PRB **47**, 14932 (1993).

$$E_{\text{PMA}} \propto (\xi)^2 \sum_{o,u,k} \frac{|\langle o, k, \downarrow | L_z | u, k, \downarrow \rangle|^2 - |\langle o, k, \downarrow | L_x | u, k, \downarrow \rangle|^2}{\varepsilon_{u,k}^{\downarrow} - \varepsilon_{o,k}^{\downarrow}}$$

$$L_x = \frac{1}{2} (L^- + L^+)$$

Large matrix element of $\langle d(x^2 - y^2) | L^- | d(yz, zx) \rangle$

Increase damping with increasing EF

The $\langle d(x^2 - y^2) | L^- | d(yz) \rangle$ increase the damping, but decrease the PMA. \Rightarrow opposite EF dependence

Summary of the third topic

First principles study on voltage control of magnetic anisotropy (VCMA) and magnetic damping in Fe/MgO interface

- For Fe/MgO(001) surface, the magnetic damping increases with increasing the electron accumulation at interface (positive EF).

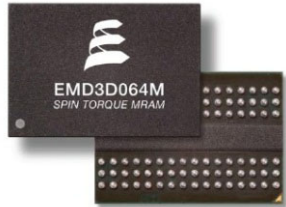
(20% of damping constant α can be changed by $E_F=1$ [V/nm] for Fe/MgO(001))

- It is opposite to that of Perpendicular MCA.

- The voltage dependence of magnetic damping of Fe/MgO(001) can be attributed to the spin conservation term.

Summary of this talk

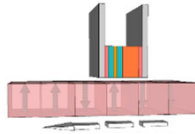
MRAM



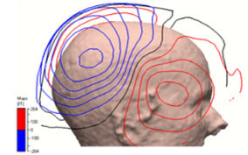
Magnetic censer



HDD read-out-head

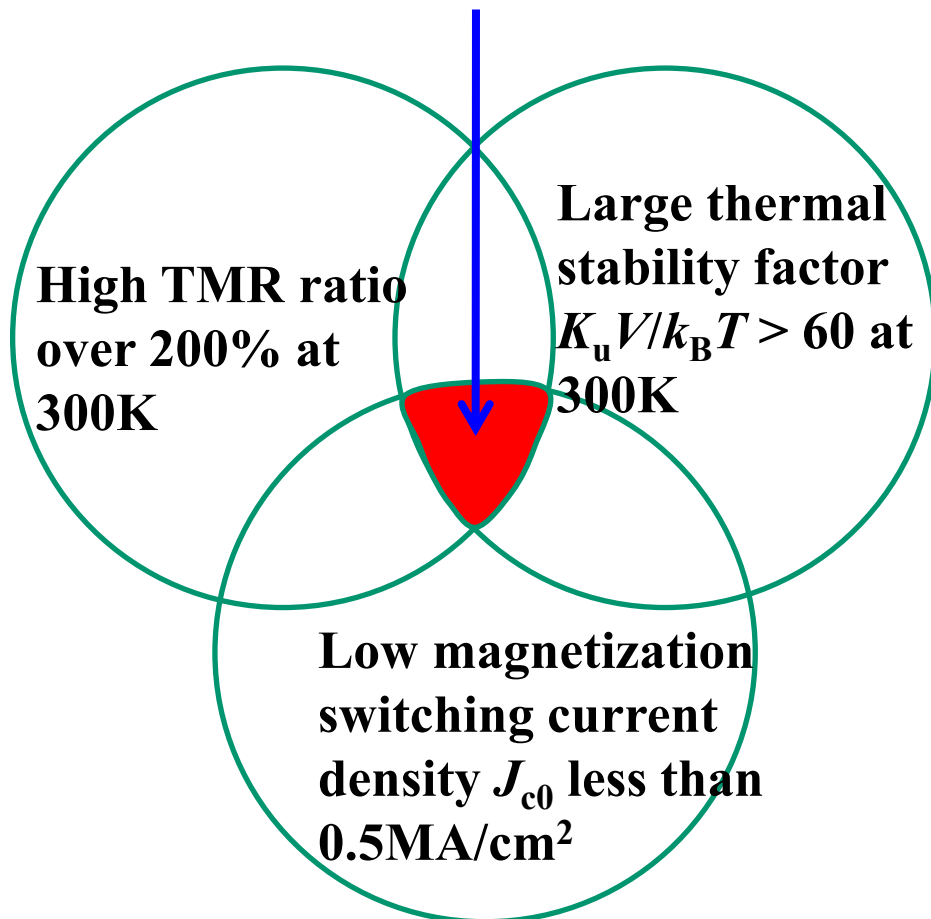


Earth's magnetic field censer • current censer for car • biomagnetic censer



Corresponding to SQUID

Required performance for pMTJs



Required properties for spintronic materials

